Comparing Performance of Different Sheet Pile Walls

by
Gongyan Gao (N)

Fourth-year undergraduate project in
Group D, 2013/2014

I hereby declare that, except where specifically indicated, the work submitted herein is my own original work.

Signature __________________________ Date ________________________

Technical Abstract

Sheet pile retaining walls are widely applied to various projects to restrain lateral soil movements. Sheet piling can offer significant advantages over other retaining structures in terms of price and ease of installation. Nevertheless, there are still drawbacks and demerits such as influence on surrounding structures during installation and large pile deflections in service. The Giken silent piler generates less noise and vibration during construction than conventional methods and Giken Seisakusho is now developing a new type of sheet pile wall named the “IP wall”, aiming to substantially reduce the lateral wall movement. Utilising the silent piling technique in constructing these stiffer IP walls will improve the popularity of sheet pile walls in the future.

Several model tests have been carried out to test the behaviour of IP wall. The model tests showed that IP wall have higher wall stiffness and will produce less head displacement than normal wall and slanting wall equivalents. In order to confirm the performance of IP wall in comparison to conventional sheet pile walls, excavation and loading tests were conducted on walls at the Akaoka test site in the summer of 2013 in Kochi, Japan. In the field test, each of the normal wall, slanting wall and IP wall was excavated to a specific depth and loaded up to maximum 800kN on a rectangular area of 18m^2 behind the wall. Data was measured by total station, strain gauges, earth pressure sensors and inclinometer. All the data after preliminary data processing gave two sets of values for earth pressure, displacement and moment alone the pile, which allows further data analysis.

The reliability of the in-situ data measuring system and collection system was verified by comparing two sets of data. The applicability of existing theoretical models, including Limit Equilibrium Design (LED) and Mobilisable State Design (MSD) was then checked with the practical field test data. Results showed that possible range of wall movement can be predicted with good accuracy using MSD using reasonable and relatively accurate input conditions. Furthermore, the extent of influence of initial shape of the pile, joint coefficient of pile, angle of friction of soil, soil type, undrained shear strength and other soil properties

on lateral deflection of sheet pile wall during excavation and loading tests were discussed in this report.

Based on the field test results, the IP wall was found to produce far less lateral displacement during loading tests in comparison to the other two walls. Nevertheless, the pre-loading stage of IP wall generates extremely large wall movements, which narrows the application of the IP wall. Extensive use of IP wall into practical projects needs to solve this problem.

Finally, further research on improving the accurate lateral displacement control under specific magnitude of pre-loading was suggested. The suggestion of more detailed investigation of initial shape and joint efficiency has been proposed at the end of the report, since they were found to substantially change the behaviour of sheet pile wall.

Acknowledgements

This project and the associated field tests were carried out with the support of Giken Seisakusho Ltd, as a part of the Giken-Cambridge collaboration. I am very grateful to Mr. Kitamura, President of Giken Seisakusho, who generously sponsored this research program. Particular thanks must go to Dr. Stuart Haigh, my project supervisor, for his teaching and helpful advice.

The assistance of Giken engineers Mr Y. Ishihara, Ms N. Ogawa, Mr K. Okada, and Mr M Lei was greatly appreciated throughout the research. I am also thankful to the Giken engineers for performing the model tests and field tests before our arrival to Japan and after our departure from Japan. The practical assistance of Mr. Nose and other Giken operators on-site has also been invaluable. In addition, a special thanks to Mr. G. Stevens for his help in inclinometer measurements, preliminary data analysis and precious ideas in discussion.

A final acknowledgement is to Professor Malcolm Bolton, Ms Burali d'Arezzo and Mr P. Shepley for general assistance and explanations during the past two years.

Nomenclature

SPT	Standard Penetration Test
CPT	Cone Penetration Test
TS	Total Station
ULS	Ultimate Limit State
SLS	Serviceability Limit State
LED	Limit Equilibrium Design
MSD	Mobilisable Strength Design
θ	Rotation of Pile
q_c	CPT Cone Penetration Resistance
f_s	CPT Sleeve Friction
u	Pore Water Pressure
N_k	Cone Factor
I_c	Soil Behavior Type Index
ϕ	Friction Angle of Soil
F_s	Factor of Safety
Sr	Degree of Saturation
e	Voids Ratio
R_f	CPT Friction Ratio
v	Specific Volume
p_a	Atmospheric Pressure
S_u	Undrained Shear Strength
c_{mob}	Mobilised Shear Stress
γ_{mob}	Mobilised Shear Strain
σ_v	In-situ Vertical Stress
σ_v'	In-situ Vertical Effective Stress
σ_h	In-situ Horizontal Stress
σ_h'	In-situ Horizontal Effective Stress
Gs	Specific Gravity of solid
γ	Unit Weight of Soil
γ_w	Unit Weight of Water
γ'	Buoyant Saturated Unit Weight
K_a	Active Earth Pressure Coefficient
K_p	Passive Earth Pressure Coefficient
q	Surcharge on the Active Side
$\gamma_{m=2}$	Strains Mobilized at Half the Peak Shear Strength (%)

Contents

1. Introduction **1**

1.1 Motivation **1**

1.2 Giken Press-in Technology **1**

1.3 Aims **3**

1.4 Theory **4**

2 Field Tests **7**

2.1 Type of sheet pile walls involved **7**

2.2 Layout of Tests **10**

2.3 Content of Tests **12**

2.4 Apparatus **12**

2.5 Methodology **14**

2.6 Site Investigation Data **16**

2.7 Problems Encountered **20**

3. Summary of Model Test Results **22**

4. Reliability of Practical Results **23**

4.1 Field Test Data by Different Apparatus **23**

4.2 Error Test on Inclinometer **25**

5. Theoretical and Practical Results **27**

5.1 Matlab Software **28**

5.2 Unit Weight **28**

5.3 Angle of friction **29**

5.4 Undrained Shear Strength **31**

5.5 Compare Theoretical and Field Test Data **32**

6. Performance of Normal Wall, Slanting Wall and IP Wall 42

7. Conclusions 44

8. Future Work 46

9. Reference 46

10. Health and Safety 49

11. Appendix 50

1. Introduction

1.1 Motivation

As a type of retaining wall, sheet pile walls are actively involved in civil constructions to retain lateral stress of soil. Around the world, steel sheet pile walls are gaining popularity as foundations, restraining soil in excavations, and as highway structure footings. Approximately 2 million tons of steel is exploited annually for sheet piles. (Smoltczyk, 2003)

Sheet pile walls are inexpensive, offer easy and rapid installation, and need no previous excavation. However, the large noise and vibration produced during construction is seriously problematic in urban areas. For steel sheet pile walls, various pile shapes can be achieved easily due to the ductility of steel, however corrosion, low efficiency of interlock and large head deflection can be its disadvantages.

Most of calculations and standards dealing with retaining wall structures are for ultimate limit state (ULS) design, for which the wall under load of failure is investigated. However the Servicability Limit State (SLS) is also extremely crucial in areas where large deflection of the pile and significant effect on surrounding environment is not permitted. To achieve extensive use of steel sheet piles, advanced press-in method to reduce noise and vibration, and new sheet pile techniques to decrease movement of the pile are required.

1.2 Giken Press-in Technology

Accompanied by rapid urbanisation, new pile installation techniques which will exert less distortion to the surrounding environment become more attractive from social and economical points of view. Increasingly stringent regulations on noise, vibration, pollution and distortion have also promoted the development and advancement in piling technology. The silent piler invented by Giken, overcomes these potential problems. The silent piler uses static load generated by hydraulic rams for press-in. As a result, it generates far less vibration and noise when compared to dynamic penetration methods which rely on percussive or vibratory energy. In addition to the static load, press-in of a pile using a Giken

Silent Piler involves utilising the extraction resistance of previously installed piles as reaction piles. The press-in mechanism is illustrated in Fig.1. The Giken silent piler is able to walk along the piles during the construction. The 'self-walking' system requires no temporary works and permits construction at constrained sites, as shown in Fig.2 (White and Deeks, 2007).

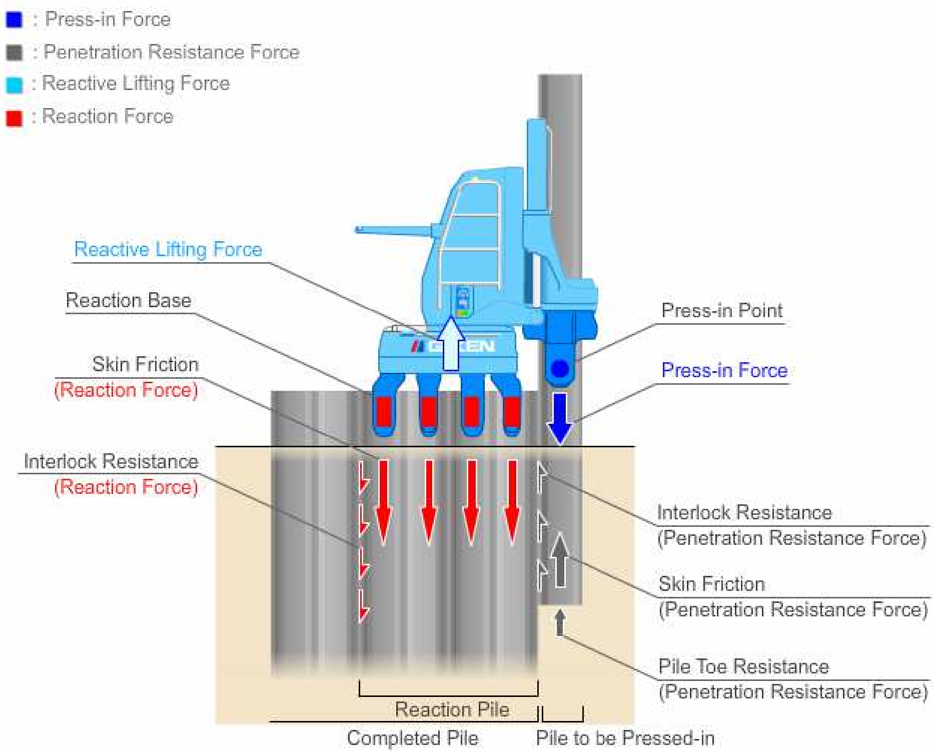

Fig.1 Press-in Mechanism of Giken Silent Piler on Sheet Piles: Interlock resistance and skin friction of previous piles act as reaction force, together with the static force by hydraulic rams, helping the installation of piles (image courtesy of Giken).

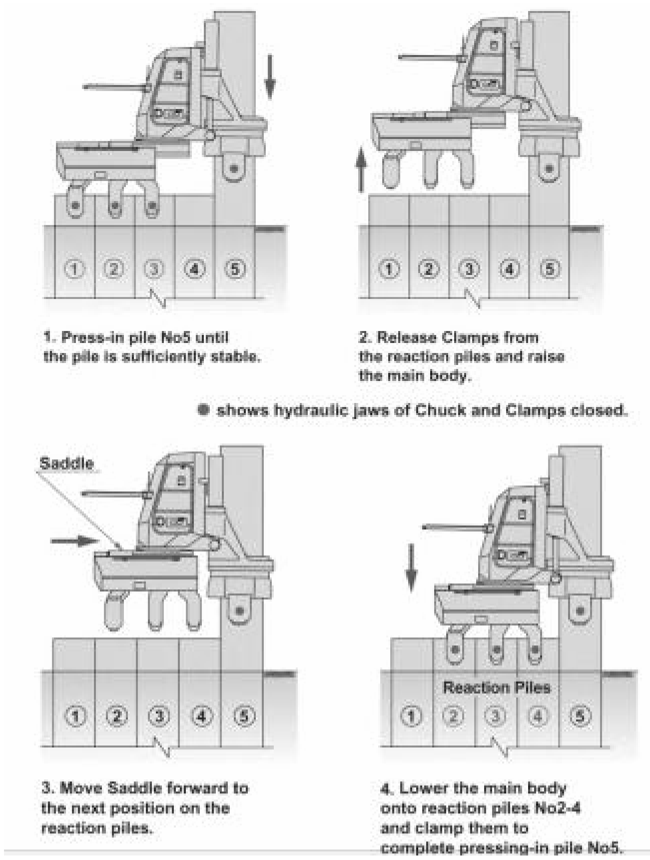

Fig. 2 'Self-walking' Mechanism of Giken Silent Piler (White and Deeks, 2007)

1.3 Aims

The purpose of this project is to explore a sheet pile wall design which suffers less lateral displacement and therefore less distortion to the surrounding. Particular attention is also given to prediction of wall movement by LED and MSD. More specifically, the report intends to

● Compare reliability and applicability of data acquisition by different apparatus

● Investigate the consistency between the existing theoretical models of displacement prediction for sheet pile walls and real field test results

● Use theoretical models to find out the degree of influence for different soil and wall parameters on the wall deflection

● Perform a comparison between different types of sheet pile walls and thus verify whether IP wall is more effective than the traditional walls

● Analyse the feasibility of IP wall and its prospects

● Identify productive areas for future research

1.4 Theory

1.4.1 Mobilisable Strength Design Method

Mobilisable Strength Design (MSD) is a unified method based on plasticity theory and mobilisable strength of soil, which can be applied for both ULS and SLS. The idea of MSD is use of admissible strain fields to model soil behaviour, which was first proposed by Bolton et al (1989). The term 'Mobilisable Strength Design' was first coined by Osman and Bolton (2004).

In this report, MSD is carried out using a Matlab program. The general procedure for MSD is listed below:

1. For a pile with known shape, γ_{mob} is calculated for the soil along the pile.
2. c_{mob} obtained from the stress-strain curve
3. Equilibrium is used to calculate pile bending moments
4. Lateral deflection is calculated based on beam theory.

These four steps are then repeated until equilibrium is achieved.

1.4.2 Mobilised Strain at Half the Peak Shear Strength $\gamma_{m=2}$

$\gamma_{m=2}$ is the strain mobilised at half of peak shear strength. MSD explores the extent of the mobilised shear strength during deformation, hence $\gamma_{m=2}$ is an extremely important parameter. Vardanega and Bolton (2011) proposed a power curve correlate the mobilised strain and the degree of mobilised strength, as plotted in Fig.3.

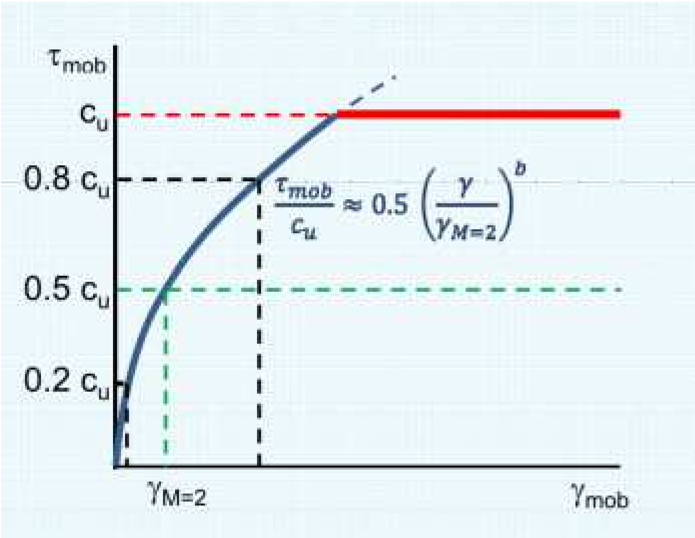

Fig.3 Relationship between Mobilised Stress and Mobilised Strain by a power curve Vardanega and Bolton (2011)

The equation $\frac{\tau_{mob}}{c_u} \approx 0.5 \left(\frac{\gamma}{\gamma_{M=2}}\right)^b$ proposed by Vardanega and Bolton (2011) represents the relationship between mobilised stress normalised by undrained shear strength, against peak strain normalised by strain at half of the peak stress, based on 115 tests on 19 different types of clay and silts. The value of b is taken as 0.6 on average for all the tests.

1.4.3 Limit Equilibrium Analysis

Limit Equilibrium Design (LED) was first developed in the 20th century. LED assumes a specific pattern of passive and active soil pressures is developed so that the overall earth pressure satisfies force and moment equilibrium. A number of earth pressure distributions for retaining walls have been proposed and started to be widely used, such as the Engel's Method and the Krey's Method.

Although these methods approves to be good approximations, the unknown parameters such as the point of zero net pressure, are relatively difficult to determine. In spite of the fact that ULS design by LED is often carried out, design procedures for SLS are not clearly stated by most standards and regulations. Instead, a factor of safety F_s is usually applied on the soil strength at SLS, to ensure that the wall is away from ULS (Diakoumi and Powrie, 2013).

1.4.4 Limit Equilibrium Approximation for SLS

In this project, wall movement at SLS estimated by LED is only an approximation using a factor of safety $F_{S.}$ Rankine's approach for a smooth wall at ULS is applied first. For cohesive soil, the equations applied are

$$\sigma'_v = \gamma z - u + q$$

Active Side: $\sigma_h = \sigma_v - 2s_u$

Passive Side $\sigma_h = \sigma_v + 2s_u$

For frictional soil, the equations involved are

Active Side: $\sigma'_h/\sigma'_v = (1\text{-}\sin\phi')/(1+\sin\phi') = K_A$

Passive Side: $\sigma'_h/\sigma'_v = (1+\sin\phi')/(1\text{-}\sin\phi') = K_P$

The smooth wall is a conservative assumption, for practical rough wall, Rankine's method for smooth wall over-predicts the wall loads and hence displacement.

After the passive and active earth pressures are determined, the force and moment on both sides can be calculated. The next step is to calculate the factor of safety F_s for moment, where F_s = Moment on Passive Side/ Moment on Active Side. The FoS of moment is used since the failure mechanism is usually controlled by moment, thus FoS of moment is the critical factor.

The lateral displacement can then be determined from Fig.4 by assuming a rigid pile rotating about its base (Clayton & Milititsky, 1986). Note that model in Fig.4 assumes that the retaining soil is sand.

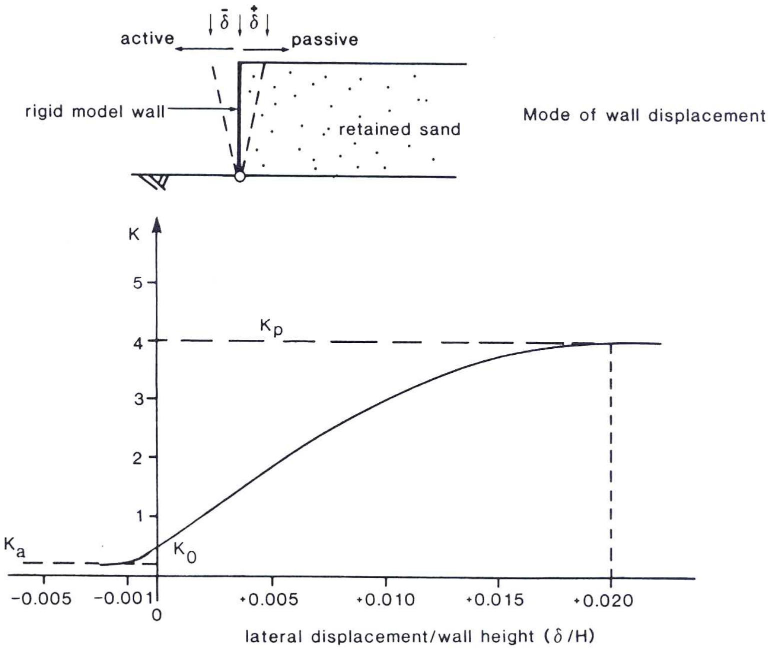

Fig.4 Variation of Lateral Earth Pressure Coefficient with Wall Movement

2 Field Tests

Three types of sheet pile walls (normal wall, slanting wall and IP wall) were tested at the Akaoka test site in Kochi, Japan from June to November, 2014. The Cambridge team were present for the normal wall test. All the piles involved were U-shaped steel sheet pile. This section presents the layout of tests, methodology and apparatus involved in the tests and properties of soil based on site investigation.

2.1 Type of sheet pile walls involved

2.1.1 Normal Wall

The normal wall is the traditional and most widely used sheet pile wall. Construction of the normal wall involves pressing the wall vertically into the soil, which is easy and quick. Nevertheless, normal wall may suffer from large horizontal displacement and large embedment depth, which significantly inflates the construction cost. To restrain the lateral displacement, short struts might be required, reducing the workability in construction

(Ogawa, 2013). Comparison between normal wall, slanting wall and IP wall is shown in Fig.5 below.

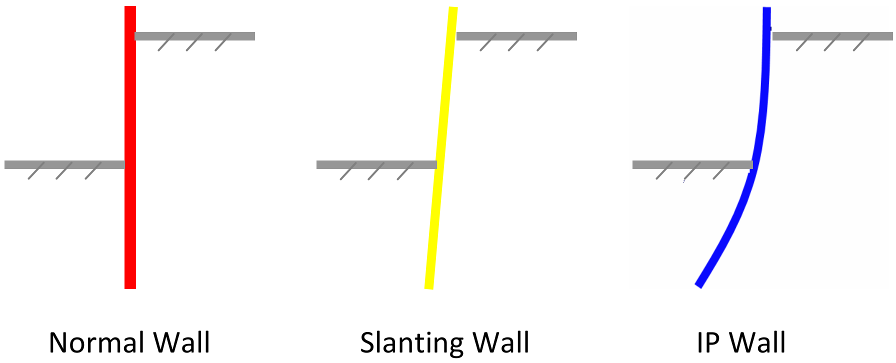

Fig.5 Comparing Normal Wall, Slanting Wall and IP Wall

2.1.2 Slanting Wall

The slanting wall is a relatively new technique and has been adopted in several recent projects. Each sheet pile is installed at a specific angle (5° in our case) from the vertical axis. In our field test, the inclination of sheet pile is achieved by rotating the piler, as shown in Fig.6. The angle of inclination is checked during the press-in process and the angle of pile head is maintained at roughly 5°.

Fig.6 Installation of Slanting Wall

Model tests by Giken Seisakusho showed that a slanting wall with an inclination of 10° suffers less horizontal displacement than a normal wall but the wall movement is still significant during excavation and loading. From a visual point of view, an initially inclined wall with reducing angle of inclination will cause less panic than an initially vertical wall that curves into the excavation.

2.1.3 IP Wall

IP wall, short for Implant Preloaded Wall, is an original idea developed by Giken Seisakusho, Japan. The IP wall is installed at an angle as for the slanting wall, followed by excavation and preload of the wall towards the excavation side. After the backside is filled with soil, the wall is unloaded. The construction of IP wall is finished at this stage. Note that the preloading was provided by jacking force, as illustrated in Fig.7.

Through preload and backfill, IP walls should have a higher initial stiffness than the other two walls owing to locked-in stresses behind the wall, and hence much lower lateral displacement are expected after completion of construction and in service. The construction procedure of the IP wall is shown in Fig.8. From the results of model tests, the additional stiffness due to preload and backfill is confirmed and it is expected that IP wall usually requires no support and struts in most cases. (Ogawa, 2013)

Fig.7 Preload of IP wall

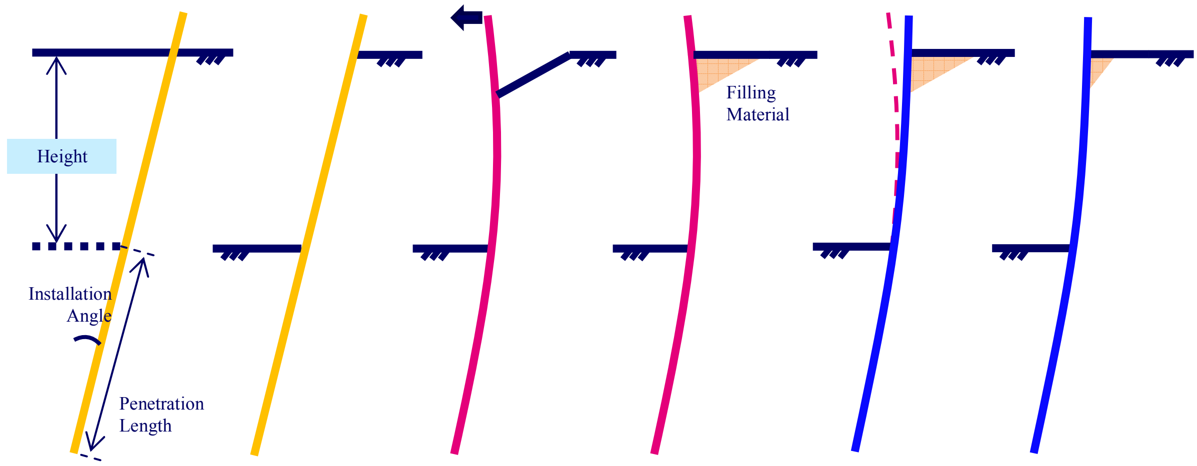

Fig.8 Construction Procedure of IP Wall (image courtesy of Giken)

2.2 Layout of Tests

All three wall tests were conducted on the Akaoka test site in Kochi, Japan. Normal wall tests, including installation, excavation, loading tests and extraction were started on June 14, 2013 and finished on August 7, 2013. IP wall tests were conducted between August 19 and October 7, followed by slanting wall tests from October 8 to November 8. From Fig.9 and Fig.10, sites for the normal wall test, slanting wall test and IP wall test are side by side and spaced 3m apart.

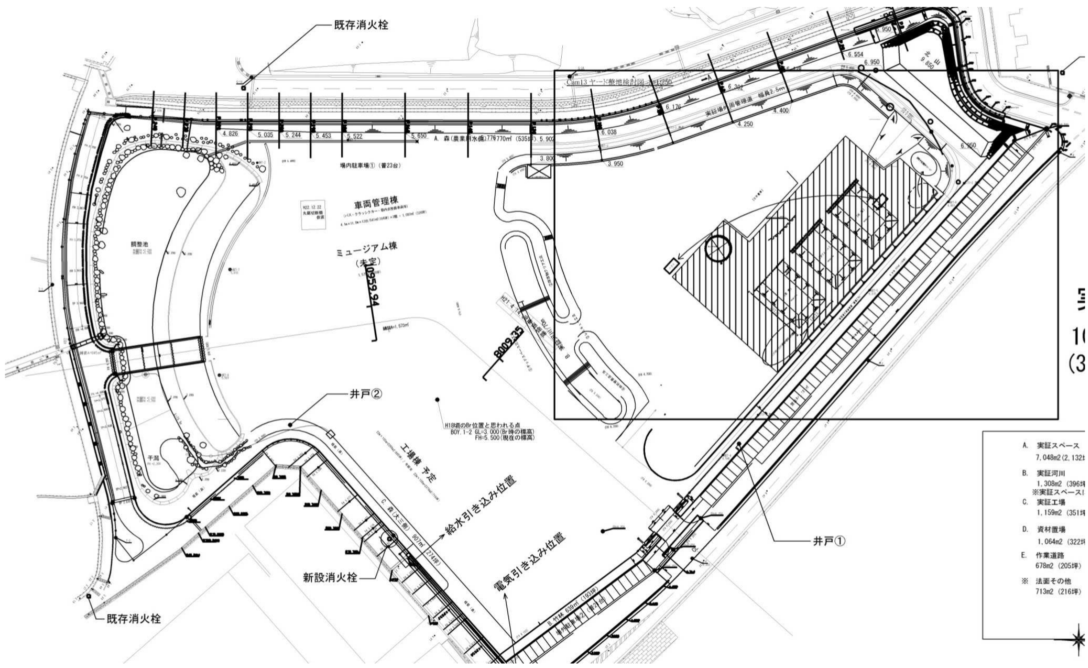

Fig.9 Layout of Akaoka Test Site (image courtesy of Giken)

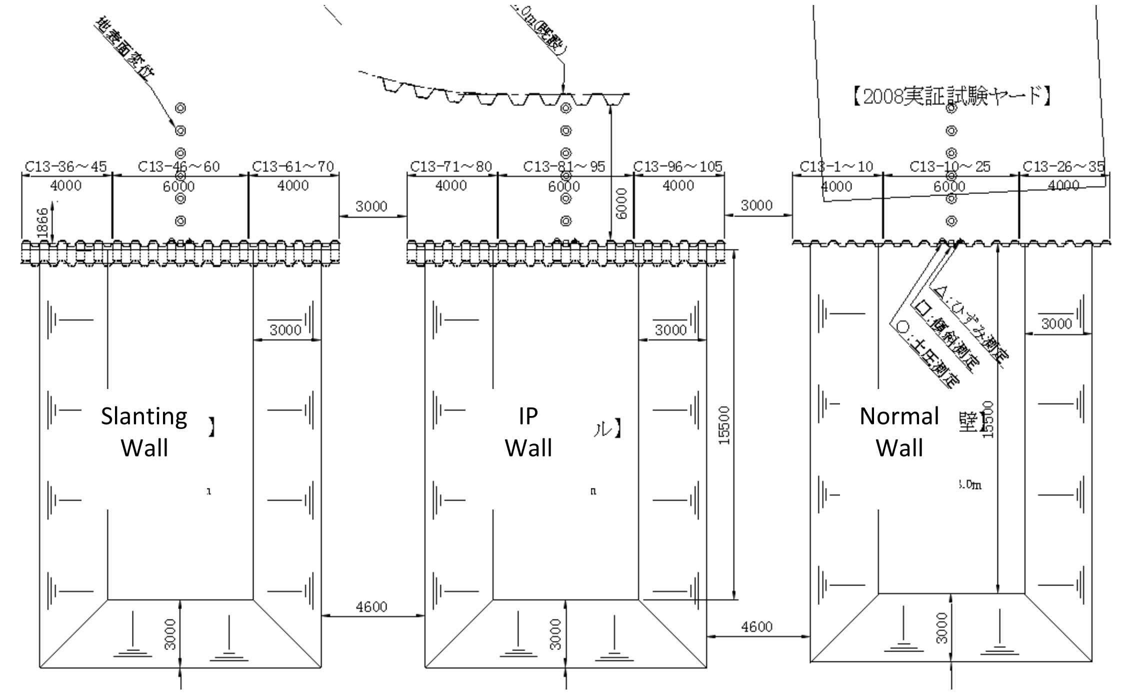

Fig.10 Layout of the Wall Tests (image courtesy of Giken)

Fig.11 shows a detailed plan of each of the test cells. Each of the walls consists of 35 piles. The middle 15 piles are test piles, interlocking with each other. On each side of the test piles, there are 10 retaining piles, separated from the test piles, as shown in Fig.12. Therefore there will be no secondary lateral displacement of test piles due to horizontal displacement of retaining piles. Other joints of the U-shaped sheet pile walls are all fully interlocked.

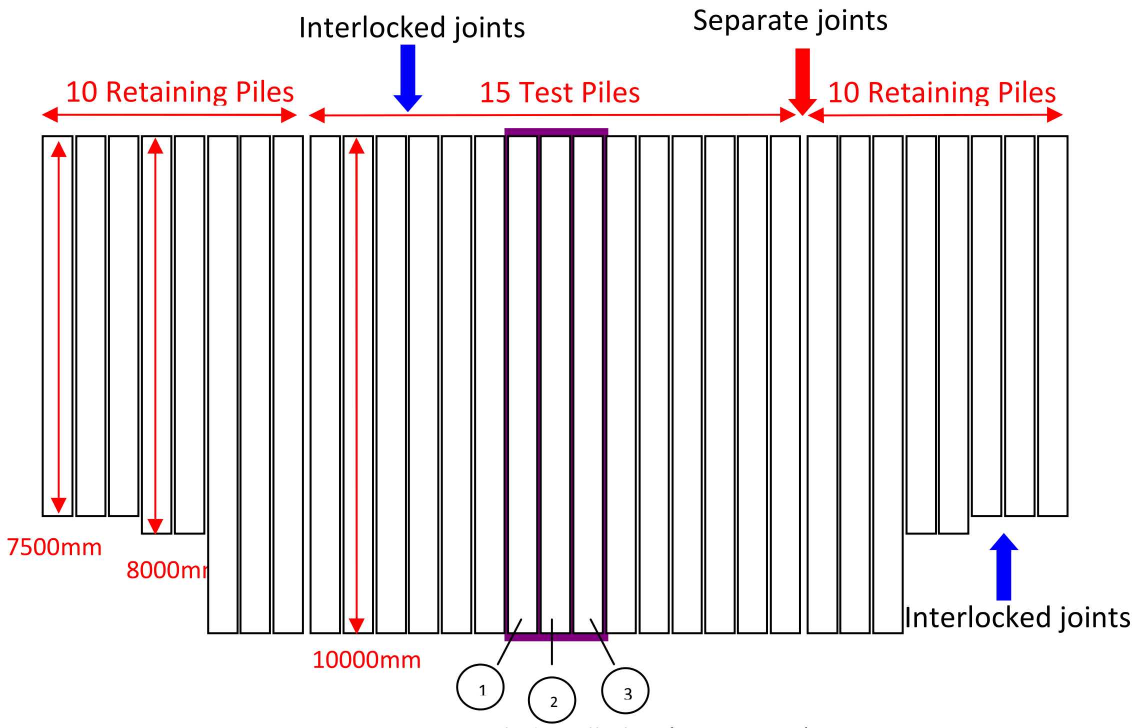

Fig.11. Detailed Wall Plan (Front View)

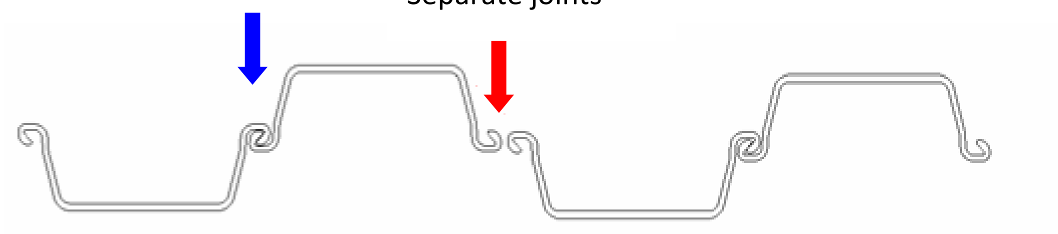

Fig.12 Interlock between piles (edited from Giken Presentation)

2.3 Content of Tests

All the three tests involve steps listed below:

1. Installation of Piles to form a sheet pile wall
2. Excavation down to a depth
3. Loading test at the specific depth
4. Extraction of the wall

The loading area is a 6m (length) x3m (width) rectangular plate 1m away from the wall.

The excavation depth and loading tests are summarised in Table.1.

	Normal	Slanting	IP
Excavation to 3m	x		
Excavation to 3.5m	x	x	x
Excavation to 4m	x		
Loading Test at 3m up to 250kN/13.9kPa	x		
Loading Test at 3.5m up to 550kN/30.6kPa	x		
Loading Test at 3.5m up to 800kN/44.4kPa	x	x (2)	x (2)
Loading Test at 4m up to 800kN/44.4kPa	x		

Table.1 Test items for normal wall, slanting wall and IP wall; x denotes for a conducted item, and (2) stands for 2 tests were done for this particular item.

2.4 Apparatus

Measurement equipment involved in the field tests are total stations (TS), earth pressure sensors, inclinometers and strain gauges. The TS is used alone while the other three measurement equipments are attached to 3 of the central test piles. The piles marked 1, 2 and 3 in Fig.11 are piles equipped with inclinometer, earth pressure sensor and strain gauge respectively. After loading tests, all the piles were extracted. All the piles except the pile with strain gauges were reused for other walls.

2.4.1 Inclinometer

Inclinometer is used to monitor deformation or movement and to measure the angle of slope. In our field tests, a square inclinometer tube with a side length of 50mm and a thickness of 3.2mm was welded to the middle of pile 1. Measurements were taken every 50mm for early tests and changed to every 20mm after excavation of the normal wall to increase the accuracy of data.

2.4.2 Earth Pressure Sensor

Four earth pressure sensors are equipped on Pile 2, at 1, 2, 3 and 4 meters below the ground level. Each sensor is chemically protected and waterproofed. The surface of the earth pressure sensor is in the same plane as the pile and hence is expected to measure the lateral pressure exerted on the pile by the soil.

2.4.3 Strain Gauge

Strain gauges are equipped every 1 meter along Pile 3. The top strain gauge is at the pile head. At each depth, 3 gauges are equipped, one at the centre and two at the sides, as shown in Fig.13 (b). An active-dummy 4-gauge system was used in the strain gauge to mitigate the error caused by temperature. It is worth mentioning that although the dummy gauge allows temperature compensation, the thermal effect across the thickness of the sheet pile can not be eliminated. Similar to the earth pressure sensors, clay and waterproof material was used to protect the strain gauges from impact and groundwater.
The arrangement of inclinometer tube, earth pressure sensors and strain gauges are shown in Fig.13.

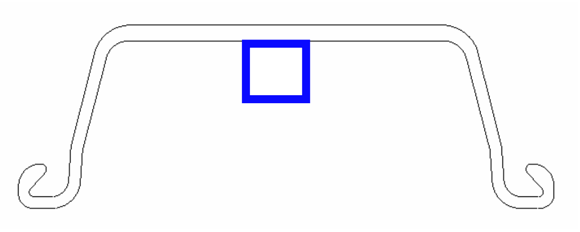

Fig13 (a) Inclinometer Tube

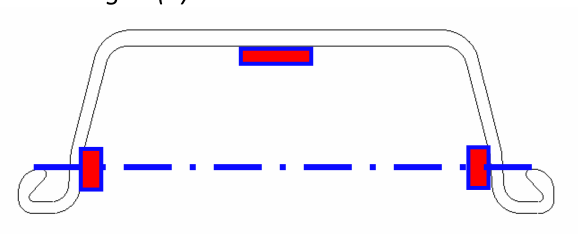

Fig.13 (b) strain gauge

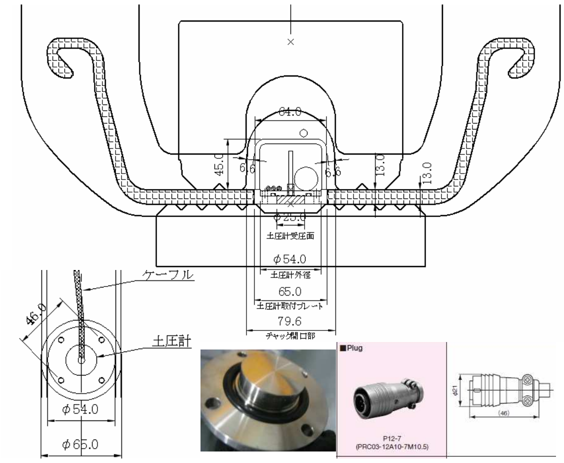

Fig.13 (c) Earth pressure sensor

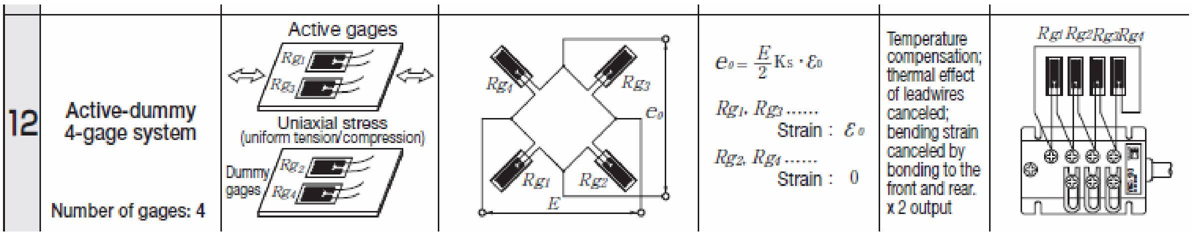

Fig.13 (d) Active-dummy 4-gauge system used in strain gauges

Fig.13 arrangement of measuring apparatus (image courtesy of Giken)

2.4.4 Data Acquisition System

The data logger, UCAM, is exploited to record the output values from strain gauges and earth pressure sensors. The UCAM is attached and detached from the pile at the beginning and completion of the tests everyday. Since the memory of the UCAM is not unlimited, the UCAM data is then saved and copied to a computer soon after the test.

2.5 Methodology

2.5.1 Reliability of Field Data

Data are collected from TS, inclinometer, strain gauges and earth pressure sensors. The inclinometer data can be differentiated and calibrated to produce moment, or be integrated to get the pile displacement. Moreover, the earth pressure data can be obtained by differentiating the pile displacement twice. Therefore, inclinometer can produce lateral displacement of the pile, moment distribution and earth pressure distribution alone the pile.

Next to the inclination pile, strain gauges are able to produce moment by using compatibility and moment-curvature relationship. Besides, TS can measure the head displacement and earth pressure sensor, by its name, measures the earth pressure.

The pile shape is thought to be continuous and smooth. Therefore, a 6^{th} order polynomial is fitted to the original displacement profile from inclinometer to obtain a smooth pile shape. Angle used for moment calculation is treated via a filtfilt command in matlab, to avoid unreasonable fluctuations in moment profile. A reasonable level of data fitting between processed data and original data was achieved.

Measurements mentioned above can produce two sets of data for each of the head displacement, moment and earth pressure respectively. Comparing the two sets of data would give a preliminary conclusion on whether the experimental data collected are reliable. However, note should be taken that the first measurement (at the bottom of the pile) of inclinometer is unreliable. Take the length of inclinometer itself into consideration, the first reliable reading from inclinometer is 8m for normal wall and 8.3m for slanting and IP wall.

2.5.2 Match of Practical Results to Theoretical Prediction

Theoretical methods including MSD and LED are used to predict the movement of the pile and moment distribution alone the pile. By calculation of LED and matlab program of MSD, the extent of fitting the experimental data with theory can be examined. This allows reliability of the measuring equipments to be checked and allows us to have a general idea about the accuracy of our field tests. Unfortunately, broken strain gauges and huge error in earth pressure sensors measurement made the comparison less valuable.

2.5.3 Influence of Soil and Wall Parameters on the Wall Movement

The Matlab program based on MSD can be run several times with different soil and wall parameters including angle of friction, unit weight of soil, joint coefficient of wall, to name but three. At each comparison, one parameter is varied and others are fixed. This allows effect of individual parameters on the lateral displacement to be visualised.

2.5.4 Compare different sheet pile walls

Moment and displacement during excavation and loading for normal wall, slanting wall and IP wall can be plotted out. Comparison of performance among the three walls should relatively direct and easy to find from the plots.

2.6 Site Investigation Data

CPT was conducted three times, near the sites of normal wall, slanting wall and IP wall respectively. Graphs of cone penetration resistance, referring to the force required to push the tip of the pile down, are drawn respectively in Fig.14.

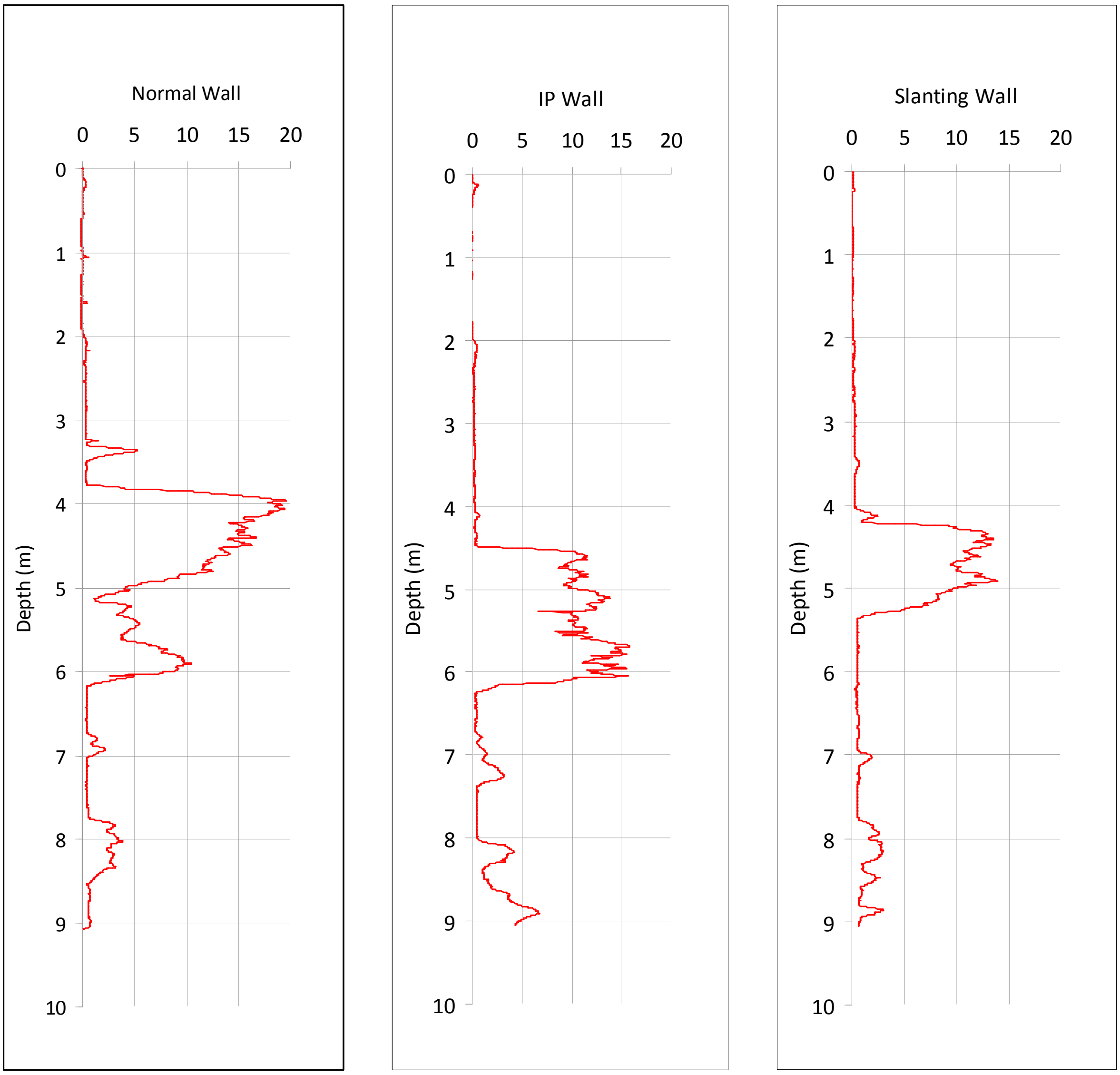

Fig. 14 Cone Penetration Resistance q_c (MPa) of Normal Wall, IP Wall and Slanting Test cells

The overall profiles for the three cells are similar, with a lower resistance for the top 4m and peak resistance from 4m to 6m and decrease to low values below 6m depth. In spite of the overall similarity, the Normal wall site experienced the highest peak resistance of about 20MPa while the peak values for other two sites are about 15MPa. Also, the middle high resistance section for IP wall is shorter, and the resistance decreases to 1MPa soon below 5.3m. This will slightly influence the prediction of friction angle for the three walls later in this paper.

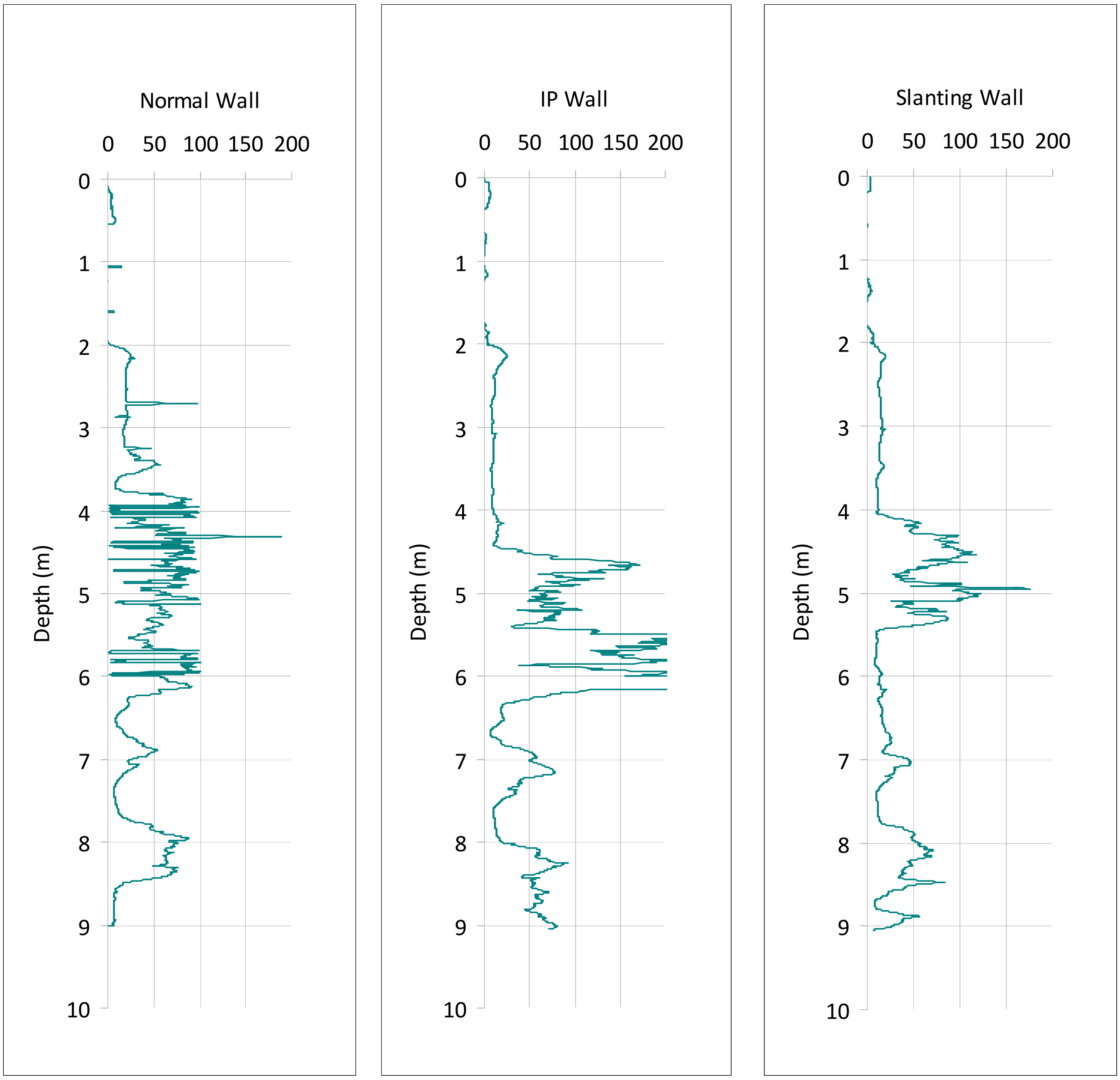

Fig.15 Sleeve Friction f_s (kPa) for Normal Wall, IP Wall and Slanting Test cells

The Sleeve friction, indicating the required force to push the sleeve of the pile down, followed a similar overall trend as the cone penetration resistance. One difference is that, sleeve friction is relatively low for the normal wall and high for the IP wall at middle depth.

Sleeve friction profiles of the three walls are shown in Fig.15. By knowing the cone penetration resistance q_c and sleeve friction f_s , 'friction ratio' R_f referring to the ratio between sleeve friction and tip friction can be determined, and soil type and resistance of the soil to liquefaction can be thereby determined.

Generally, sand gives high end resistance and low friction ratio, while clay is more likely to have a low end resistance and thus high friction ratio. From Fig.14 and Fig.15, soil on normal wall site tends to have a higher tip resistance and a lower friction ratio, which is more sand-like.

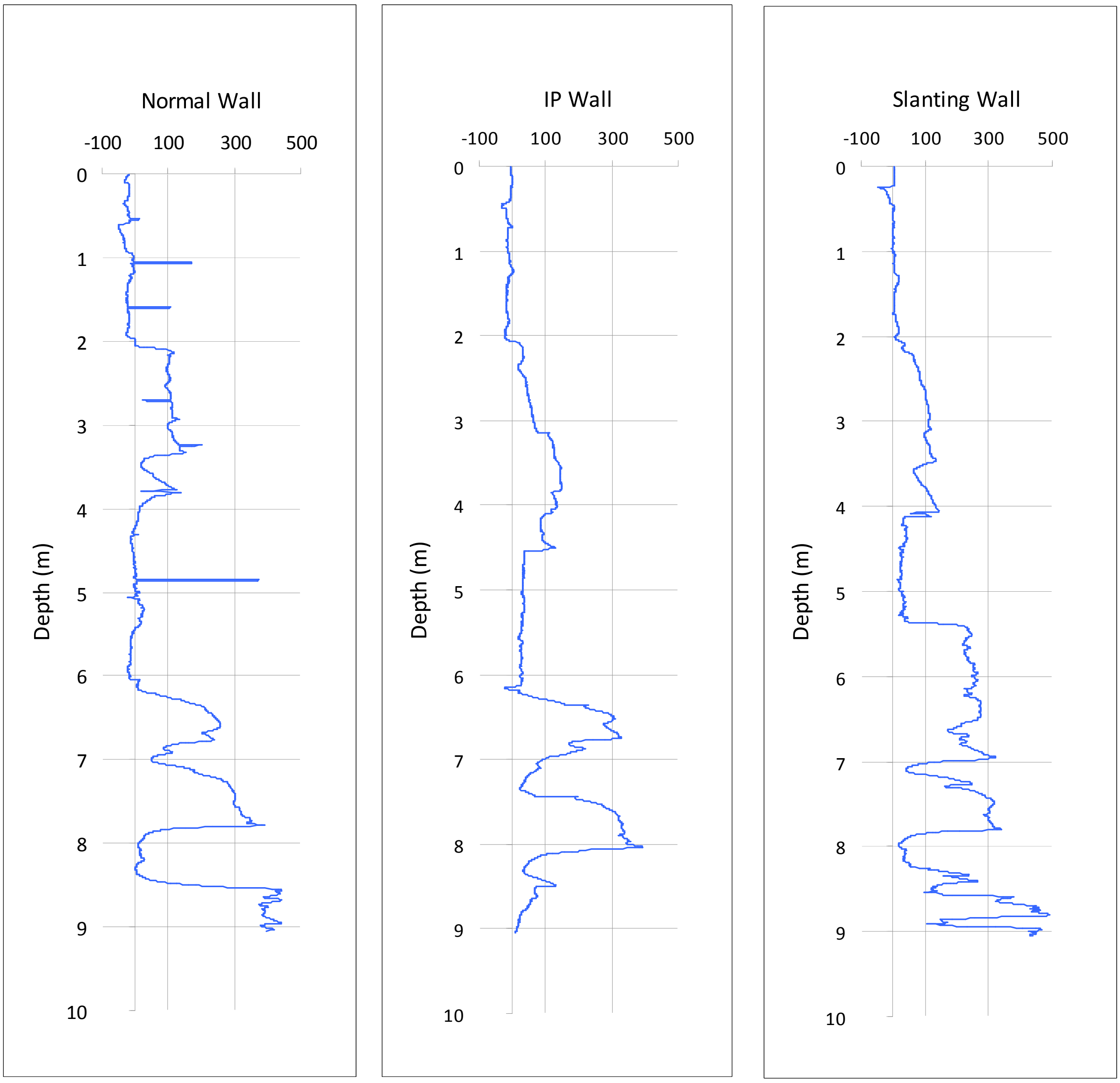

Fig.16 Pore Water Pressure u for Normal Wall, IP Wall and Slanting Test cells

Pore water pressure is simple and direct. From Fig.16, pore water pressure for all three sites start to increasing significantly at about 2m. A suitable guess would be the water level is around 2m at the time the CPT tests were conducted. However, this only shows the water pressure distribution on a particular day, and no obvious trend for a hydrostatic pressure distribution can be detected from the graph.

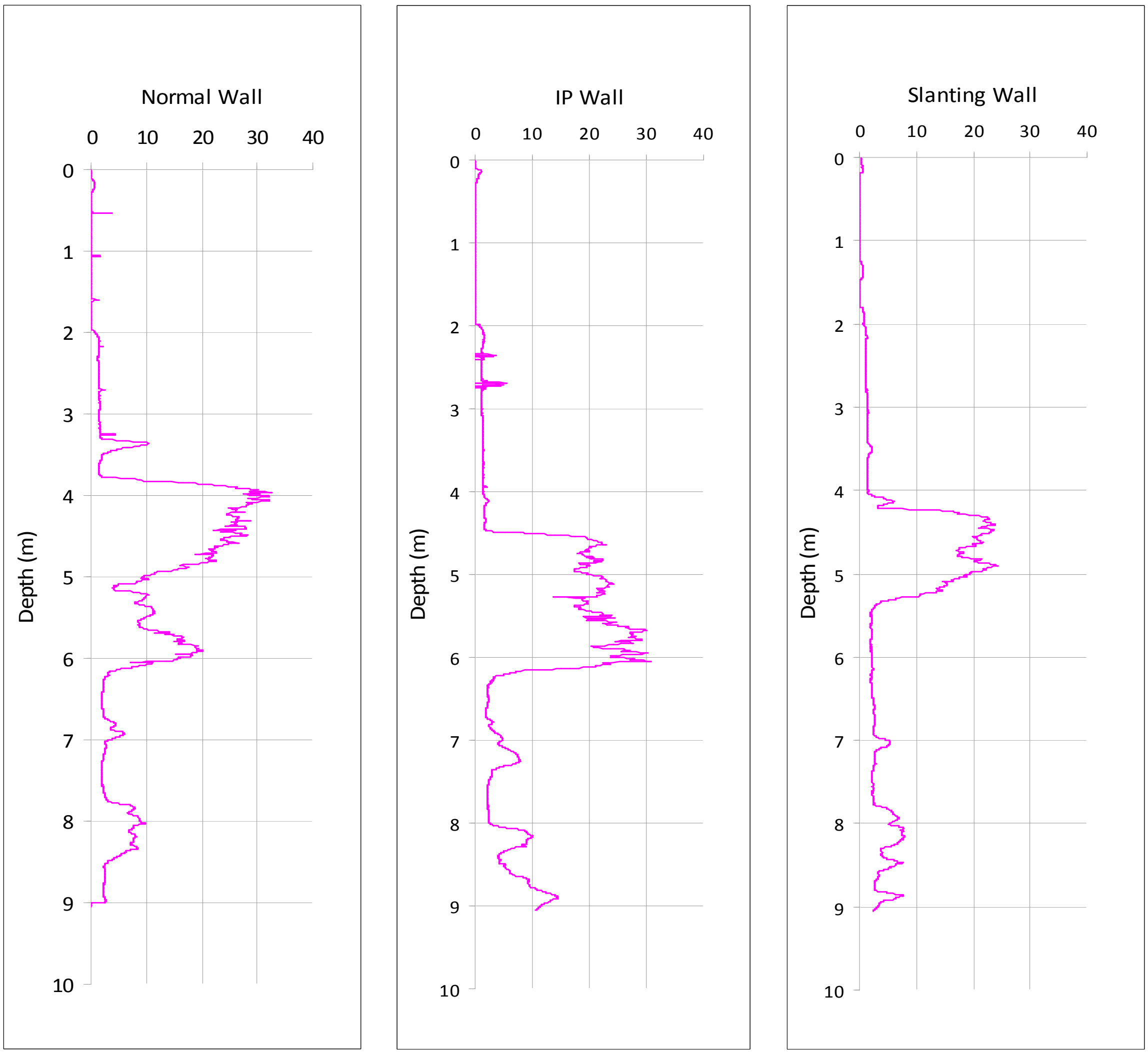

Fig.17 N-value for Normal Wall, IP Wall and Slanting Test cells

The SPT N-value is defined as number of standard blows required for a specific distance of penetration. It is widely accepted as an indication of soil density and soil type. An equivalent N-value can be derived from cone penetration resistance q_c from a CPT test, proposed by Jefferies and Davies (1993). Equivalent N-values for the normal wall site, IP wall site and slanting wall site are plotted in Fig.17. Sand with an N-value less than 30 can be classified to have a loose to medium relative density. Clay with an N-value greater than 8 can be classified as stiff. From Fig.17, top sand is loose while sand in the middle layer is relative dense. Bottom clay is medium to stiff in terms of consistency.

According to Robertson (1990), soil type can be determined based on cone penetration resistance q_c and friction ratio from CPT measurements. The figure used is in Appendix. For convenience, soil type of every 1m depth is deduced, shown in Table.2. This is consistent with the friction ratio that soil on normal wall site is more sand-like.

Depth	Normal	Slanting	IP
0-1	sand	sand	sand
1-2	sand	sand	sand
2-3	clay	clay	clay
3-4	silty sand	clay	clay
4-5	gravel	silty clay	sand
5-6	sand	sand	silty clay
6-7	clay	clay	clay
7-8	clay	clay	silty clay
8-9	clay	silty clay	silty clay

Table.2 Soil Type for Normal Wall, Slanting Wall and IP Test cells

In the top 2m, all the three test cells are filled with sand, which can be considered to be drained in both short term and long term. In the middle layer (2m- 6m), soil is frictional or cohesive. In the bottom 3m, the soil is clay or silty clay, which can be considered to be drained in long term but undrained in short term.

2.7 Problems Encountered

A few numbers of problems and difficulties were encountered during the field tests.

● Most of the strain gauges on the normal wall and some of the strain gauges on the slanting wall and IP wall are broken during the installation of pile under the earth pressure and the press-in force. The closer to the pile tip, the greater the earth pressure and the press-in force was acting during installation. Therefore most of the broken strain gauges were close to the pile tip.

Learning from the strain gauge failure of normal wall, the protective paints of strain gauges on IP wall and slanting wall was thickened. As a result, more strain gauges on IP wall worked well. However, all the strain gauge readings for slanting wall were incredibly large. Whether this was due to an electronic error, twist of the sheet piles or any other possible reasons has not been determined yet.

The status of strain gauges for normal wall and IP wall are shown in the table below.

No.	Normal Wall			IP Wall		
	L	C	R	L	C	R
1	o	o	o	o	o	o
2	o	o	o	o	o	o
3	x	o	x	x	x	o
4	x	o	x	o	o	o
5	x	x	x	o	o	o
6	x	x	x	o	x	o
7	x	x	x	o	x	o
8	x	x	x	x	o	x
9	x	x	x	x	x	o
10	x	x	x	x	x	x

Table.3 Status of strain gauges for normal wall and IP wall; x represents broken strain gauge, o represents strain gauge in good condition; L represents for strain gauge in left hand site, while C and R stands for centre and right respectively.

● Inclinometer readings were taken every 50mm initially. However, inclinometer data is not sufficiently precise and accurate, especially where difference of angle is needed, such as moment calculation. After excavating the passive side of normal wall to 3m, inclinometer readings were taken every 20mm. This has improved the accuracy of readings. Nevertheless, in order to calculate the wall movement relative to initial value, normal wall readings need to be converted to original scheme.

● Kochi experienced several strong typhoons in September and October. Heavy rains might change the water level to a great extent, and probably led to some lateral displacement change in IP wall and slanting wall.

● Test procedures and items are not exactly the same for normal wall, slanting wall and IP wall, which made the direct comparison more difficult. The difference is due to lack of experience during normal wall tests. Loading test of normal wall at 3m up to 250kN/13.9kPa gave a displacement which is not large enough compare to the possible error in measurement. Further depth of excavation and loading test with a larger maximum surcharge was then decided, in order to achieve larger wall movement. Slanting wall and IP wall followed similar procedure and therefore is of larger comparability.

3. Summary of Model Test Results

Model tests on normal wall, slanting wall and IP wall has been conducted by Giken members before our arrival in Japan. The steel sheet pile and soil were replaced by Acrylic resin and silica sand. The model set-up and model parameters are shown in Fig.18.

	Normal Wall	Slanting Wall	IP Wall
Installation Angle	0°	10°	
Preload	0kg		5, 8kg
Height	220mm		
Overburden Pressure	0 - 7kPa (0 - 175kg)		

Fig.18 1-D Model Test of normal wall, slanting wall and IP wall (image courtesy of Giken)

Results from model test was obvious and confirmed that pre-loading is able to increase the stiffness of the wall and hence reduce the head displacement in service, as shown in Fig.19. Also, a larger pre-loading will give a stiffer wall. At a normalised pre-load being 0.95, the stiffness of IP wall was 4.5 times more than the normal wall stiffness.

The model test offered an overall idea about how an IP wall was likely to behave in field. The match of model test results to theories stimulated the field tests to be carried out.

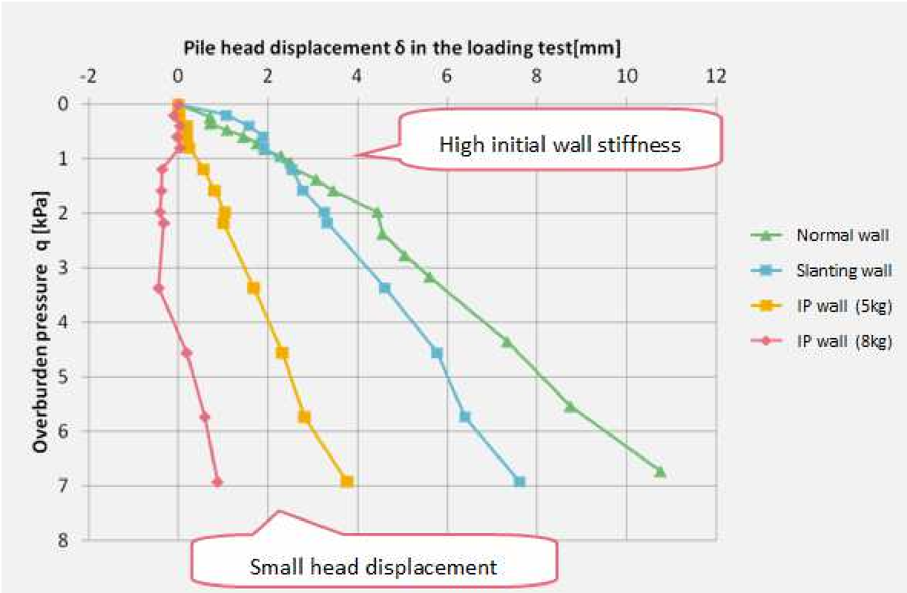

Fig.19 Displacement against sruchage for normal wall, slanting wall and IP wall (image courtesy of Giken)

4. Reliability of Field Test Data

4.1 Field Test Data by Different Apparatus

As mentioned in Methodology Section, measurements for each of the head displacement, moment and earth pressure were taken by two different apparatus to increase the reliability of data. The comparison of displacement from inclinometer and TS, and of moment from inclinometer and strain gauges are plotted in Fig.20 below.

A brief insight into Fig.20 (a) reveals that TS and inclinometer data were of good consistency. Displacement measured by TS completely matched that of inclinometer down to a 1.5m excavation level. In the following excavation and loading tests, displacement by TS is 3-5mm larger than that by inclinometer. This might come from three possible sources. The first source is error in TS measurement. Since there is no fixed point to set the TS, measurement is taken at slightly different position everyday rather than exactly the same point. The possible error caused by position of TS can be as high as 2.5mm. Excavation from 1.5m down was not on the same day as excavation down to 1.5m, which contributes to the error. Secondly, the target of TS was on the pile next to the inclinometer pile. Twisting of the sheet pile wall might result in different displacement on consecutive piles. To support this assumption, Inclinometers measurements were taken in direction parallel to the wall, which approved that the wall underwent displacement in the parallel direction. Moreover, for the inclinometer, an assumption has been made that the pile tip does not move. Sliding of the pile might account for the head displacement change in TS, but inclinometer results did not take movement of pile bottom into consideration.

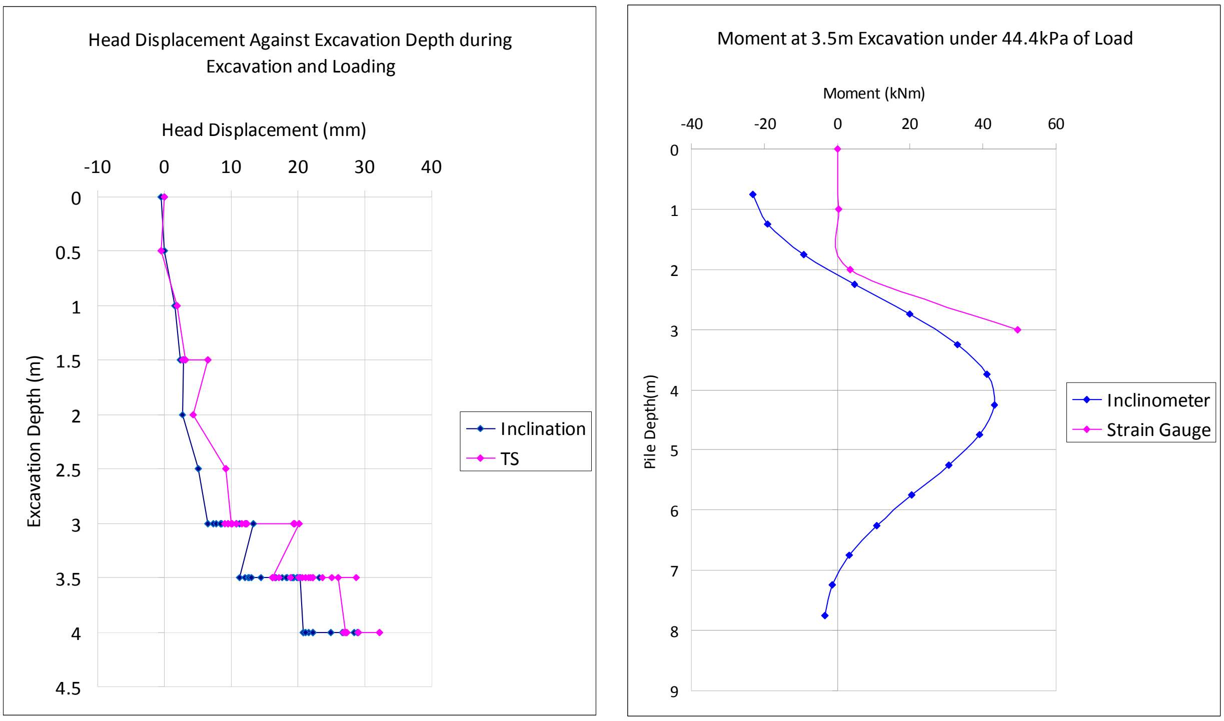

Fig.20 (a) (left) Normal wall head displacement against excavation depth during excavation and loading; (b) (right) Normal wall moment at 3.5 excavation under 44.4kPa of load alone the pile; data from central strain gauges used; only strain gauges on the top survived

In Fig.20 (b), inclinometer and strain gauges shows a similar trend, but moment calculated from strain gauge tends to peak at a higher value. The top part of inclinometer results is unreliable since moment supposes to be zero at the top of the pile. Since moment calculation explores change in angle, after filtering by the Matlab filtfilt command, the angle from inclinometer is less original. From this point of view, moment produced by strain gauge is more reliable.

Unfortunately, the earth pressure sensors did not work well in the field tests. Since the pressure change caused by shape change of the sensor might far more significant than that caused by force of soil, no sensible data was collected from the earth pressure sensor in our experiments. Earth pressure derived from inclinometer involves differentiation of the displacement, which is not of great accuracy either.

Results for slanting wall and IP wall follow a similar trend. Overall, displacement from TS and inclinometer highly agree to each other. On the other hand, moment from inclinometer and strain gauge follows same trend but give different peak values. Both inclinometer and TS appeals to be good estimation of displacement while strain gauge results are more reliable for moment calculation.

4.2 Error Test on Inclinometer

Precision of inclinometer measurements are crucial in this project, since inclinometer is responsible for all three of displacement, moment and earth pressure. Measurements under same conditions were repeated for 4 or 5 times and the difference in inclinometer output was plotted as Fig.21.

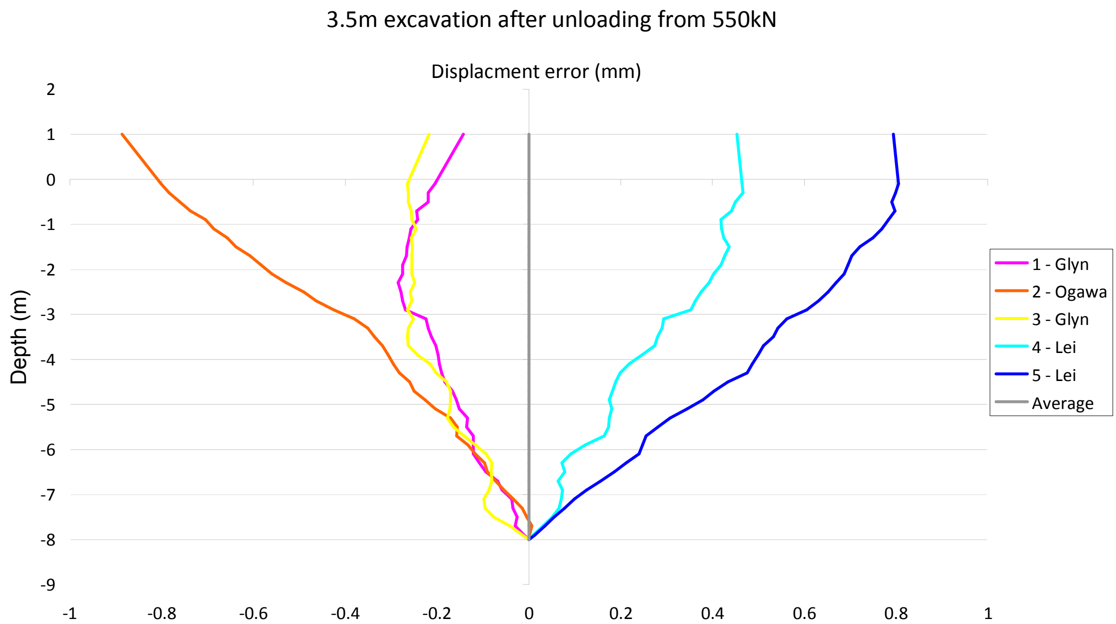

Fig.21 Results of 5 inclinometer measurements at 3.5m excavation 15 minutes after unloading from 550kN, measurements taken by different people; Error is calculated based on the average value.

From Fig.21, the maximum difference of the 5 measurements in head displacement is more than 1.5mm which is of significant error compared to a total head displacement of 7.5mm at 3.5m excavation for normal wall. Measurements taken by same people (Measurement No.1

and No.3 by Glyn and Measurement No.4 and No.5 by Lei) tend to be less different to each other. This indicates that human error is not negligible, especially when displacement is small. However, inclinometer measurements of slanting wall and IP wall were taken by Okada alone. Since the wall movement is calculated based on the initial value, error due to individual habit can be eliminated in slanting wall and IP wall results. Normal wall inclinometer measurements were taken by Okada and Glyn together, where error due to individual habit needs to be taken into account.

Another possible reason of large error might be lack of waiting time. After unloading, sufficient time is required before movement fully take place. Take the bottom clay into consideration, the required time could be much more than 15 minutes, and thus displacement was still changing while the measurement were taken. However, unloading should result in a negative wall movement. Here, a positive relative displacement was seen in later measurements, which is not expected to be caused by the time problem.

Another two error tests were done on a rainy day and a sunny day respectively, 30 minutes after loading and unloading actions, all measurements taken by Glyn, plotted in Fig.22 and Fig.23.

On a rainy day, the difference displacement measurements was expected to be larger since change in water level would results in consequent change in soil pressure and thus lateral displacement. However, Fig.22 and Fig.23 shows a maximum error of 0.43mm on rainy day and of 0.9mm on a sunny day. This means duration of 4 to 5 times of measurement will not change the wall displacement greatly due to the rain, and a single measurement on rainy day should be reliable as well. Compare Fig.21 and Fig.22 to Fig.23 also represents the importance of measurements consistently taken by same people.

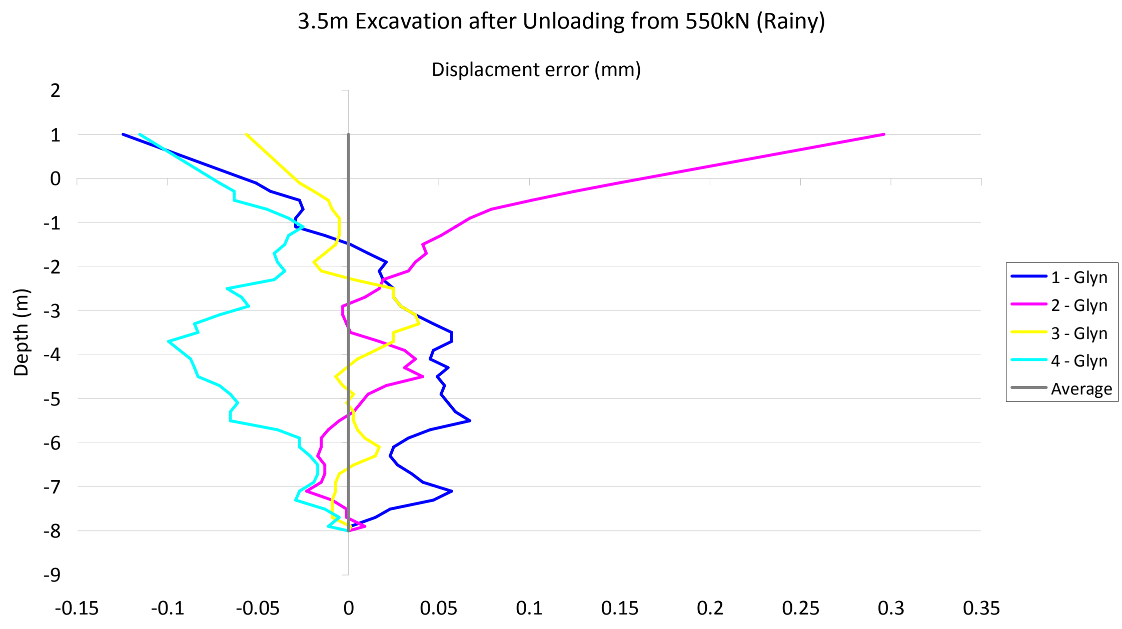

Fig.22 Results of 4 inclinometer measurements at 3.5m excavation 30 minutes after unloaded from 550kN on a rainy day, all measurements taken by Glyn; Error is calculated based on the average value.

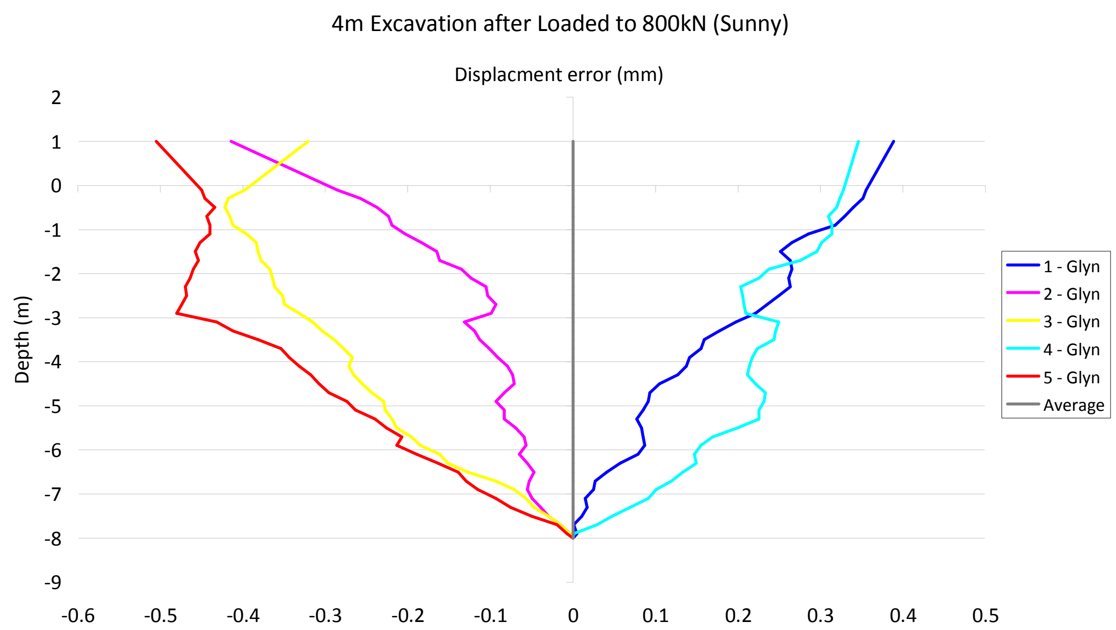

Fig.23 Results of 5 inclinometer measurements at 3.5m excavation 30 minutes after loaded from 600kN to 800kN on a sunny day, all measurements taken by Glyn; Error is calculated based on the average value.

5. Theoretical and Field Test Results

This section aims to investigate how the existing theories match the field test data for normal wall, slanting wall and IP wall. Although slanting wall and IP wall is designed to be 5°

inclined from vertical axis, the inclination angle is too small to make significant difference in soil stress. In theoretical analysis, all the walls are considered to be straight and vertical. Theoretical predictions are mainly based on a Matlab model developed by Haigh (2014), which is mobilisable strength design based. Limit equilibrium analysis is applied when considering the effect of water level.

5.1 Matlab Model (Mobilisable Strength Method)

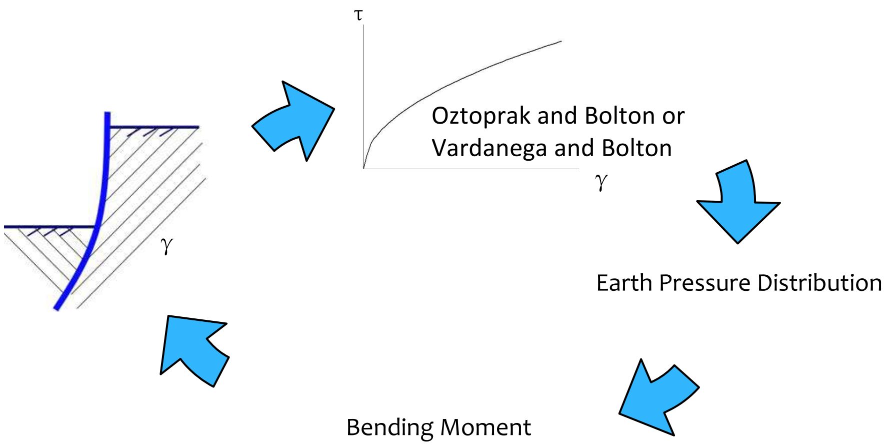

Fig.24 Principle of the Matlab Model based on Mobilisable Strength Method

Basically, as shown in Fig.24, a deformed shape of the pile is assumed first, and the shear strain γ is calculated from the shape. Shear stress τ is then determined from the shear stress-strain curve by Oztoprak and Bolton for sand and from curve by Vardanega and Bolton for clay. Earth pressure distribution can be calculated from the shear force experienced. By multiplying the Earth pressure by correct lever arm, bending moment through the pile can be determined, which can be used to calculate the deformed shape of the pile. Note that all the calculations are based on MSD method. Iterate until the results converge, and then the moment, deformed shape (pile displacement) of the pile, and earth pressure alone the pile can be deduced and plotted out.

5.2 Unit Weight

Soil type significantly varies with depth of soil, and it is difficult to measure soil weight at every depth. Instead, the one dimensional compression λ-k model was used for estimation, results in an approximate unit weight of soil to be 16-18kN/m^3 at the top and 18-20kN/m^3 at the bottom. Values of λ, k and Γ are approximated by London Clay and Weald Clay, which is over-consolidated, being similar to soil on Akaoka test site. The equations used in calculation are given as follows:

$$v = N - \lambda ln\sigma_c$$

$$\gamma = \left(\frac{G_s + S_r e}{1 + e}\right)\gamma_w$$

$$v = 1 + e$$

Value of unit weight of soil can be correlated to CPT results as well, using the following equation P.K. Robertson and K.L. Cabal (2010):

$$\frac{\gamma}{\gamma_w} = 0.27 \log R_f + 0.36 \log\left(\frac{q_c}{p_a}\right) + 1.236$$

This equation gives a unit weight of soil ranging from 16kN/m^3 to 20kN/m^3 for all three sites.

In following analysis, unit weight will be considered to be 16kN/m^3 at the top 4m, 18kN/m^3 for the middle layer of 2m, and 20kN/m^3 for the bottom 3m, for estimation.

5.3 Angle of Friction

Angle of friction, is an important measure of shear strength under drained condition. Magnitude of friction angle depends on soil type as well as density and contact of the soil.

Friction angle can be directly correlated from the cone penetration resistance according to Eurocode7, of which is shown in the Appendix. Angle of friction for three test cells is derived from cone penetration resistance accordingly, tabulated in Table.4. For simplification, the top 6m of soil is assumed to be frictional and bottom 3m is assumed to be cohesive in all three test cells.

The lateral displacement and moment for normal wall, slanting wall and IP wall is expected to be different from each other due to the different profile of friction angle, as plotted in Fig.25.

Normal Wall				
depth	qc	φ	soil	modified φ
0-1	0	29	sand	29
1-2	0	29	sand	29
2-3	0.2	29	clay	26
3-4	3	32	silty sand	29
4-5	15	39	gravel	41
5-6	6	35	sand	35
6-7	1	30	clay	27
7-8	1	30	clay	27
8-9	2	31	clay	28

IP Wall				
depth	qc	φ	soil	modified φ
0-1	0	29	sand	29
1-2	0	29	sand	29
2-3	0.2	29	clay	26
3-4	0.4	29	clay	26
4-5	12	38	sand	38
5-6	4	34	silty clay	31
6-7	1	30	clay	27
7-8	1	30	silty clay	27
8-9	2	31	silty clay	28

Slanting Wall				
depth	qc	φ	soil	modified φ
0-1	0	29	sand	29
1-2	0	29	sand	29
2-3	0	29	clay	26
3-4	0.4	29	clay	26
4-5	7	36	silty clay	33
5-6	14	38	sand	38
6-7	0.5	29	clay	26
7-8	1.6	31	clay	26
8-9	3.5	33	silty clay	30

Table.4 Friction Angle Profile of Normal Wall, Slanting Wall and IP Wall cells

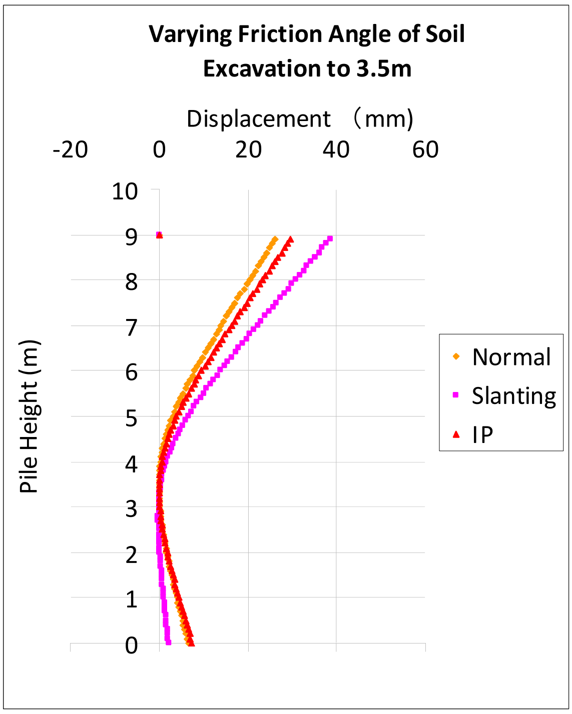

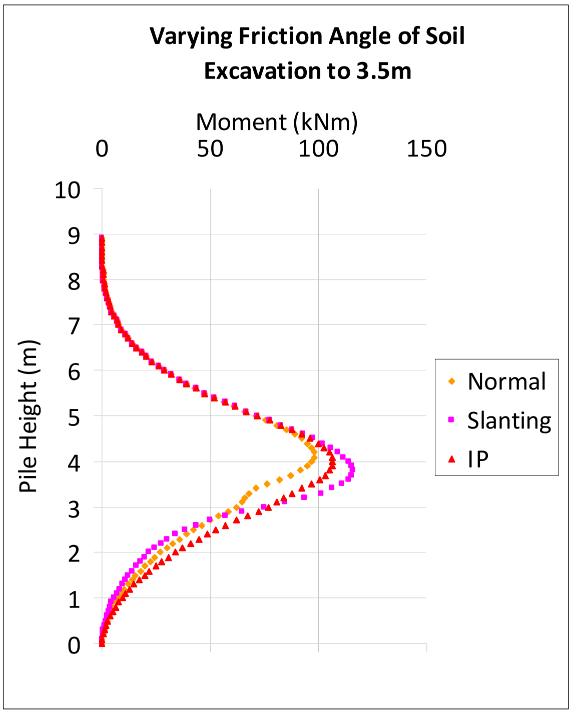

Fig.25 Compare Displacement (left) and Moment (right) at an excavation down to 3.5m and no external load applied; unit weight of soil is assumed to be as assumed in section5.2, undrained shear strength as will be described in section 5.4, joint efficiency of pile assumed to be 100%, a=0.88;g_e=7e-6 g_r=4.4e-4, b=0. a,b, g_e and g_r are soil parameters which will be discussed in section 5.5.4.

Normal wall site is of a high friction angle overall, and hence is expected to experience less lateral displacement, which is consistent with the Matlab program. The pile bottom of normal wall and IP wall is sliding away from the origin. This is due to their low value of S_u, for which a larger extent of passive strength was mobilised.

From Fig.25, angle of friction was found to be influential on lateral displacement. The test cells are about 20m apart. The friction angle profiles and thus the pile displacement profiles experience substantial variability within relative small distance. It is therefore not surprise that variation in angle of friction also exists in each of the test cell. In the following analysis, an average friction angle and undrained shear strength is picked for the three cells, as tubulised below.

<table>
<tr><th>Depth (m)</th><th>Friction Angle (°)</th><th>Undrained Shear Strength (kN/m^2)</th></tr>
<tr><td>0-1</td><td>29</td><td rowspan="6">Frictional</td></tr>
<tr><td>1-2</td><td>29</td></tr>
<tr><td>2-3</td><td>26</td></tr>
<tr><td>3-4</td><td>27</td></tr>
<tr><td>4-5</td><td>37</td></tr>
<tr><td>5-6</td><td>35</td></tr>
<tr><td>6-7</td><td>27</td><td rowspan="3">Su=74 kN/m^2</td></tr>
<tr><td>7-8</td><td>27</td></tr>
<tr><td>8-9</td><td>29</td></tr>
</table>

Table.5 Average values of friction angle and undrained shear strength for normal wall, slanting wall and IP wall test cells

5.4 Undrained Shear Strength S_u

Although the friction angle of the soil has been determined based on CPT results and Eurocode 7 in section 5.3, it is worth noting that bottom part of the soil for all three test cells are mainly clay. For clay, replacing the friction angle φ, undrained shear strength S_u plays a vital role. Undrained shear strength S_u of clay can be calculated from CPT results as well, using

$$s_u = \frac{q_c - \sigma_v}{N_k}$$

Usually N_k = 15-16 for normally consolidated clay on average

18-19 for over consolidated clay on average

Nevertheless, the values given above are just average values. Many authors have proposed that N_k for clay is usually varying within the range of 10 to 20 (Lunne and Kleven 1981, O'Riordan et al. 1982, Stark and Juhrend 1989). In this report, N_k = 18 is assumed, since the Akaoka test site is slightly over-consolidated.

Based on the CPT outputs, values of S_u for bottom 3 meters in three test cells are calculated in the table.6.

	Normal Wall	Slanting Wall	IP Wall
q_t (MPa)	1.24	2.10	1.11
S_u (kN/m^2)	61	108	53

Table.6 Values of undrained shear strength for three test cells based on CPT data

5.5 Comparing Theoretical Predictions and Field Test Data

In this section, experimental results of displacement and moment will be compared with theoretical predictions by MED and LED. Data used for displacement is based on inclinometer since TS data only measures head displacement, which does not allow us to compare the deformation of the whole pile. Moment used will be based on strain gauge and inclinometer since inclinometer does not give very reliable number and unbroken strain gauge only monitors a limited length of pile. Data shown in this report is focused on displacement, which is more reliable and direct in comparison to moment.

It is also important that theoretical predictions can not be made without knowing specific parameter about the soil and the pile. Unfortunately, it would be extremely difficult, and sometimes even impossible to measure some of the parameters directly. Instead, a reasonable value range of a parameter was proposed and curves of displacement and moment with particular values within the range were plotted. At the same time, the influence of different factors is checked by the Matlab program.

5.5.1 Effect of Initial Shape

Despite the effort to install the sheet piles straight, obvious initial bend still exists for slanting wall and IP wall, as plotted in Fig.26. The normal wall is not perfectly vertical and IP wall is more than 5° of inclination from vertical wall, but this will only give very minor change of behaviour. Normal wall is initially bent towards the excavation side, which will not be a problem since relative displacement is used during calculation. However, the slanting wall and IP wall are curved towards the active side. This will lead to extra lateral displacement since the pile springs back to straight when the excavated soil is removed during excavation.

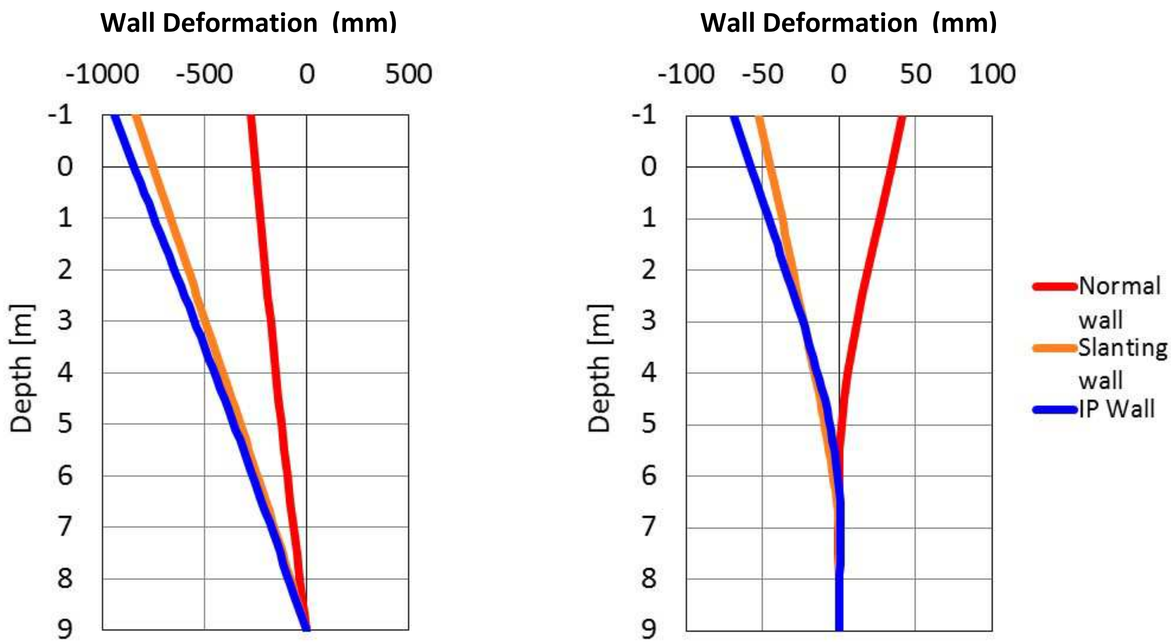

Fig.26 (a) (left) Initial shape and (b) (right) initial bend for normal wall, slanting wall and IP wall, where +ve wall deformation represents movements towards excavation (image courtesy of Giken).

From theoretical analysis, the pile starts to curve out at a depth of 5.5m at an excavation depth of 3.5m. The 5.5m is termed the level of fixity. To take the effect of initial wall shape into account, displacement due to bend of slanting wall and IP wall above 5.5m is subtracted from the final field test results, of which is plotted in Fig.27. After subtraction, the wall movement during excavation down to 3.5 becomes 10mm, 14.4mm and 5.3mm respectively for normal wall, slanting wall and IP wall. These results are not necessarily accurate since the height of soil influenced by the initial bend can not be measured and value used here is based on the guess of level of fixity. Actually, the displacement after subtraction is far too small. This means that the initial bend may not have a large height of influence. However,

Fig.27 is an important evidence to show that with a large height of influence, initial curving can strongly effect the lateral displacement. Take the large initial bend in IP wall as an example, the wall movement could potentially change by 28mm, which is substantial.

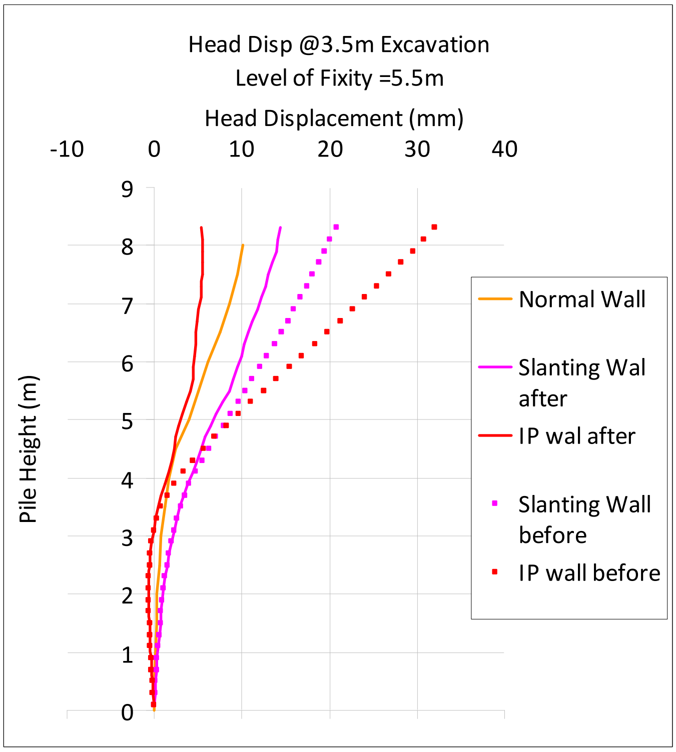

Fig.27 Normal wall, slanting wall and IP wall after subtraction due to initial bend at a level of fixity of 5.5m. Normal wall displacement is assumed to be unchanged.

5.5.2 Effect of Unit Weight of Soil

The unit weight profile from CPT and hand calculation was mentioned in section 5.2. However, this is still an estimation of unit weight of soil. The effect of varying unit weight of soil is plotted in Fig.28.

From Fig.28, varying unit value does have an effect on the head displacement but the influence is not sufficiently substantial to cover all the difference in deflection for three walls. Increasing unit weight of soil from 16 to 20kN/m3 was found to have an effect of increase the head displacement by about 4mm, about 13% of the total displacement. In addition, the theoretical curve follows same trend as the practical results, which adds reliability to the Matlab program based on MSD.

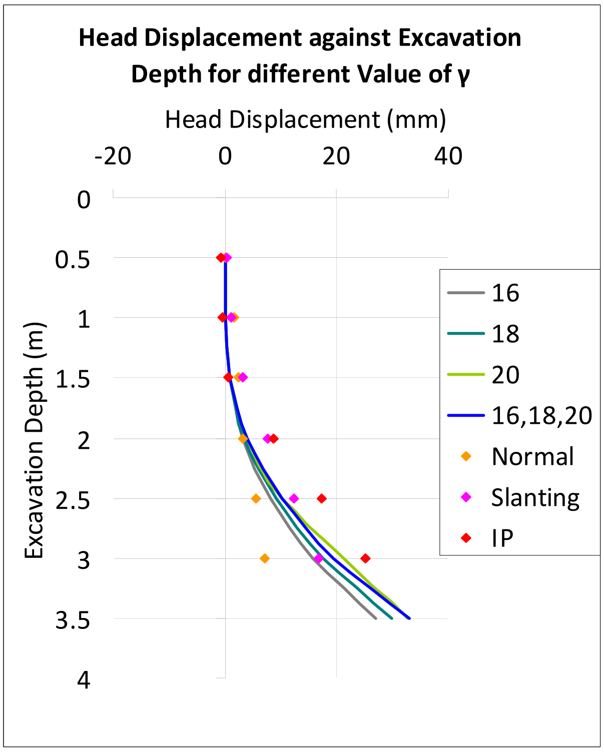

Fig.28 Head displacement against excavation level for MSD prediction and field test data. Theoretical predictions made with different values of λ.

5.5.3 Effect of Undrained Shear Strength

The average value of S_u was determined in section 5.4. Relatively significant variation in S_u can be detected in a small area. Therefore it is necessary to check how S_u will make a difference on lateral displacement. The results are plotted in Fig.29 (a) and 30 (a). Note that the inclinometer assumes displacement is zero at a pile height of 1m for normal wall, and at 0.7m for slanting wall and IP wall. The head displacement from inclinometer is added by the displacement at these levels, which shifts the inclinometer results to the right.

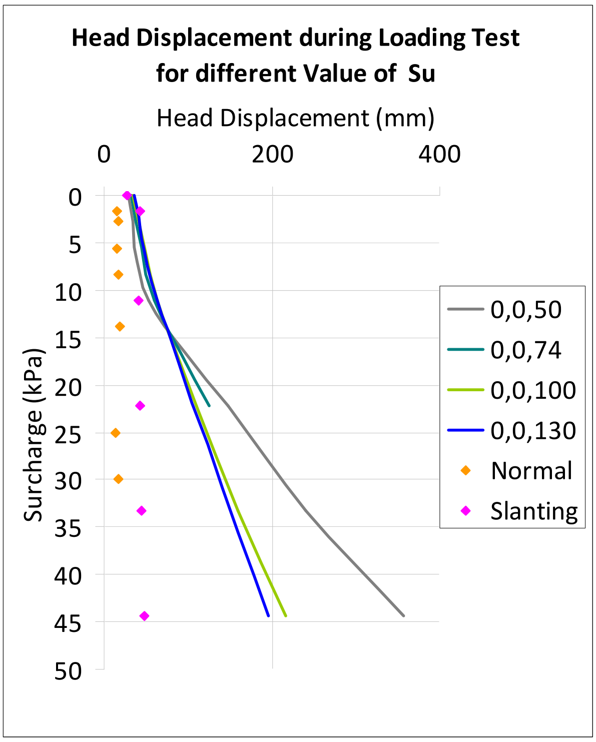

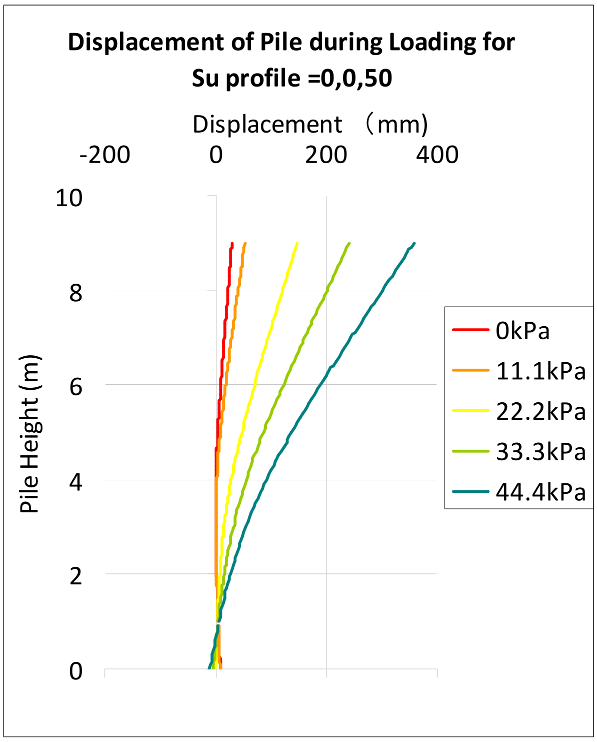

Fig.29 (a) (left) Head displacement against surcharge for MSD prediction and field test data. Theoretical predictions made with different values of S_u. (b) (right) Theoretical prediction of displacement alone the pile during loading with S_u for bottom clay equals to 50kN/m^2.

From the Fig.29, varying undrained shear stress significantly changes the head displacement during loading. It is rational that lower undrained shear stress results in larger displacement. Nevertheless, with any value of $S_{u,}$ over-estimations are made for the loading tests, as predicted values are always far larger than experimental results. In this case, the Matlab software predicts that at 44.4kPa of loading, the head displacement can be as high as 350mm at a low S_u value. Even with S_u equal to 130kPa, the head displacement at 44.4kPa loading will be around 200mm, which is not sensible in real case. The software concludes to be over-estimating the displacement during loading. A valuable point from Fig.29(b) is that, the wall is expected to rotate about a point 1m above the pile tip, which is consistent with the assumption used in inclinometer calculation.

In comparison to the loading tests, excavation tests give a good level of fit, as plotted in Fig.30.

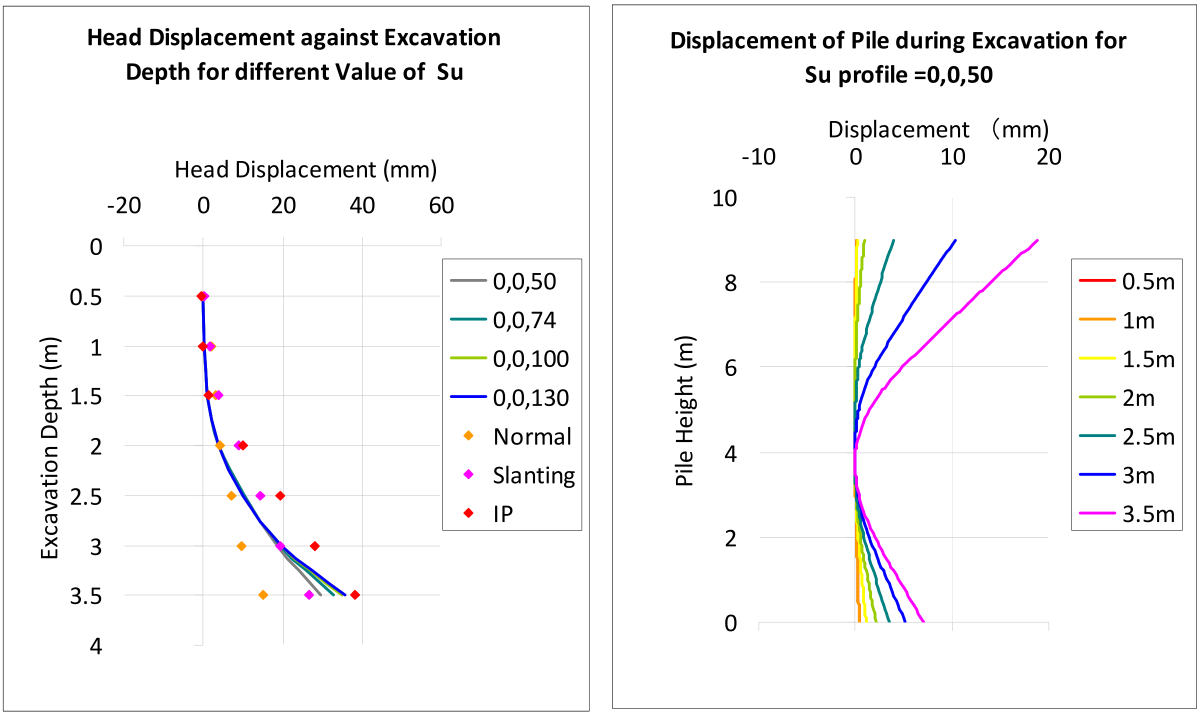

Fig.30 (a) (left) Head displacement during excavation for MSD prediction and field test data. Theoretical predictions made with different values of S_u. (b) (right) Theoretical prediction of displacement alone the pile during excavation with S_u for bottom clay equals to 50kN/m^2.

From the graph, varying undrained shear stress of the bottom cohesive soil slightly changes the head displacement during excavation, mostly at the pile tip. This is because only bottom soil is assumed to be clay in our model. With any value of $S_{u,}$ a rational prediction is made, being consistent with practical results.

Also worth noting is the shifting of pile tip during excavation, as plotted in Fig.30 (b). This might be caused by low S_u at the bottom. With low value of S_u, passive side needs to mobilise a higher fraction of ultimate strength, and higher stress mobilised might be the reason for the positive displacement at the bottom. At 3.5m excavation, the kick of the toe to the right is around 7mm which is significant. This makes the shape of the pile not very sensible in practice. Measurements from Inclinometer did not indicate a direction change in displacement at 5m below the ground level either.

Overall, undrained shear strength is not likely to change the head displacement to a large extent during excavation but make a large difference in loading test. In addition, lower S_u could possibly shift the pile bottom towards the excavation level during excavation.

5.5.4 Effect of other soil parameters in MSD

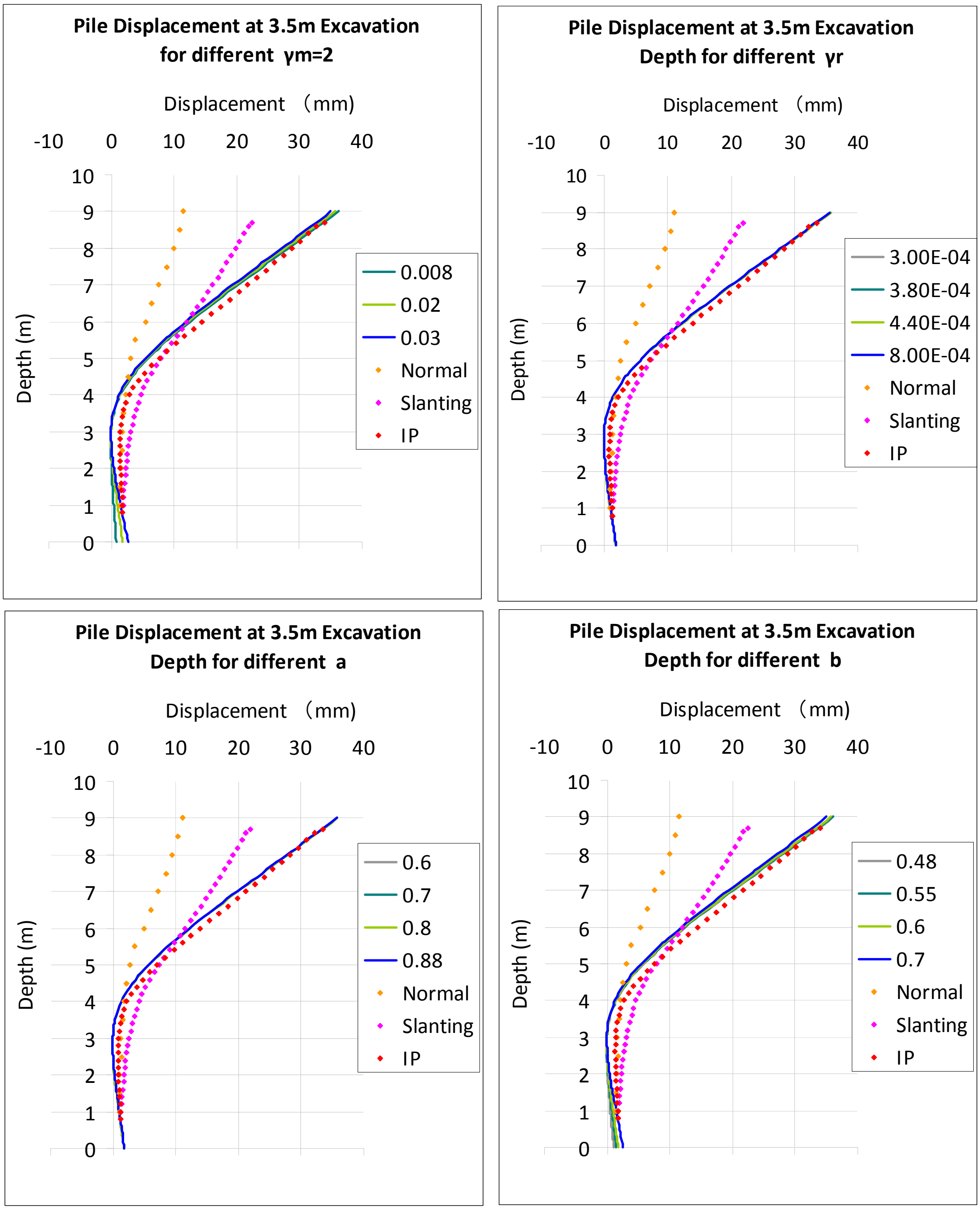

Fig.31 Pile displacement at 3.5m excavation with no applied load with different values of a, b, γ_r and $\gamma_{m=2}$.

In the above sections, the influence of friction angle and unit weight has been considered. However, there are still other parameters, which are difficult to measure, but can still effect the lateral displacement of soil. In MSE, the following equation is used to determine the mobilised friction angle:

$$\phi_{mob} = \frac{5760\gamma}{1.6^2\left(1 + \left(\frac{\gamma - \gamma_e}{\gamma_r}\right)^a\right)}$$

γ_e Is extremely small compare to γ, and hence can be ignored. The influence of the four parameters of soil, γ_r, a, b and mobilised strain at half peak strength $\gamma_{m=2}$ are examined, as shown in Fig.31 above. All of the four parameters were found to have very limited influence on the wall movement.

Besides, the theoretical prediction of lateral deflection alone the pile during excavation fits well with the IP wall, but less consistent with the slanting wall and normal wall. However, this gives a conservative prediction which is safe to apply.

5.5.5 Effect of Joint Efficiency

In previous analysis, the efficiency of joints was assumed to be 100%, which represent full EI of the pile was used to predict the displacement. Nevertheless, according to M. P. Byfield and R. J. Crawford (2003), oblique bending could take place on U-shaped steel sheet pile and result in a reduction in the EI value. The maximum possible reduction can be up to 50%. The effect of joint efficiency was analysed and plotted in Fig.32. From the graph, 50% of reduction in EI value would further shift the wall by 20mm at its head, which proves that the efficiency of joints does influence the displacement greatly. From Fig.32, a joint efficiency close to 100% should be achieved but the actual value of efficiency can be hardly measured or controlled.

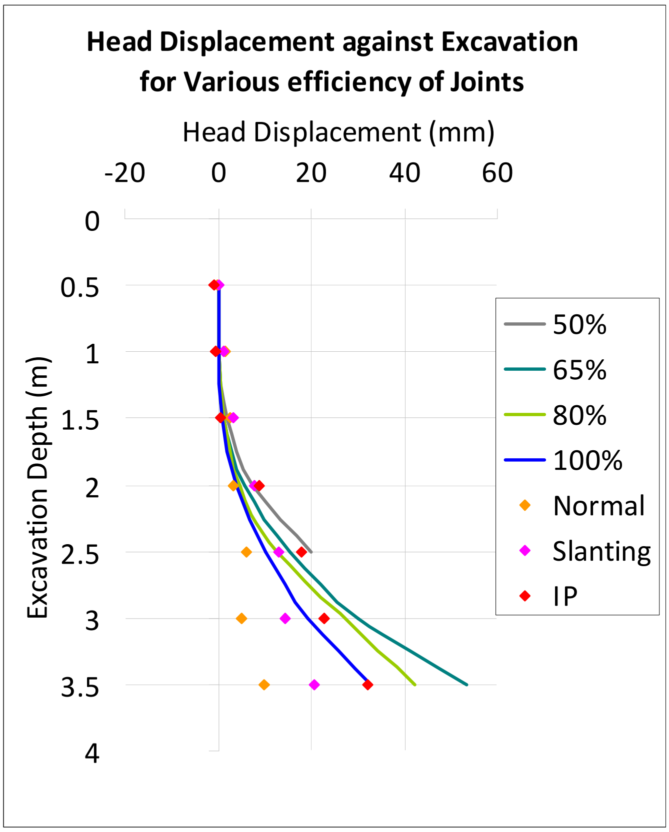

Fig.32 Head displacement against excavation level for MSD prediction and field test data; Theoretical model applied with different fraction of EI

5.5.6 Effect of Water Level

The effect of water level was examined by using limit equilibrium analysis based on the assumption that the sheet pile is under rigid rotation about pile tip. The calculation is all about soil stress analysis with a pressure head difference, coved in section 1.4.3 and 1.4.4. By substituting φ=29 for top 4m, φ=37 for 4m-6m, and S_u = 120kPa for bottom 2m, the anticipated lateral deflection with varying water level is shown in Table.7 and Table.8 below.

Water Level at what depth below the soil at active side	FoS (Force)	FoS (Moment)	Gamma (disp/L)	Head Displacement (mm)
0m	4.56	1.61	0.008	72
1m	4.94	1.76	0.007	63
2m	5.27	1.94	0.006	54
3m	5.53	2.13	0.005	45
3.5m	6.63	2.36	0.004	36

Water Level at what depth below the soil at active side	FoS (Force)	FoS (Moment)	Gamma (disp/L)	Head Displacement (mm)
0m	2.65	0.99	0.020	180
1m	2.52	1.01	0.019	171
2m	2.57	1.06	0.016	144
3m	2.71	1.13	0.014	126
3.5m	2.66	1.15	0.0125	113

Table.7 and 8. Expected head displacement based on limit equilibrium design under 3.5m excavation (top) and 800kN loading (bottom) by assuming ϕ=29 for top 4m, ϕ=37 for 4m-6m, and S_u = 74kPa for bottom 2m.

The field test data shows that, under 3.5m excavation:

Normal Wall: 10mm; Slanting Wall: 20.8mm; IP Wall: 32mm (Not considering initial shape)

Normal Wall: 10mm; Slanting Wall: 14.4mm; IP Wall: 5.3mm (Considering initial shape)

Under 800kN of load: Slanting Wall: 55mm (Not considering initial shape)

Slanting Wall: 48.6mm (Considering initial shape)

Normal wall data does not exists since loading of normal wall is up to 550kN. Head displacement of IP wall is not under the scope of this analysis since change in head displacement is significant during preload but very minor during loading.

Pictures taken on site shows that water level of three sites when excavating down to 3.5m were: Normal Wall:3m; Slanting Wall: below 3.5m; IP Wall: below 3.5m

This gives a deflection of 45mm for normal wall, and less than 36mm for slanting wall and IP wall during excavation, which is an overestimation for normal wall and reasonable for the other two. The results from LED for loading are definitely larger than the field test results. This could be caused by the assumption that the graph from Clayton & Milititsky (1986) is applicable to sand only. For clay which has a higher stiffness, the displacement is expected to be smaller. In addition, the rigid pile assumption is far from true in real tests.

5.5.7 Theoretical and Practical Results

Based on the graphs and analysis in section 5.5, with a sensible set of parameters (joint efficiency=100%, a=0.88; g_e=7e-6 g_r=4.4e-4, friction angle =average value of three cells, unit weight of soil varies from 16 to 20kN/m^3 from top to bottom), the Matlab program results in good estimation during excavation but it is likely to over-estimate wall movement during loading. Lines of predictions on excavation follow similar trend and shows kind of average behaviour of the practical data, which proves the reliability of the software for excavation.

Predictions by LED for sand tend to over-estimate the displacement in most of the case. With more experimental specimens, the factor of over-estimation can be deducted and the analysis can be more valuable.

Moment is more complicated than displacement. Moment calculated from inclinometer peaks at similar depth but at lower magnitude compared to the predicted values from the software. Strain gauges follows similar trend as predictions but only parts of the data from strain gauges are available.

6. Performance of Different Sheet Pile Wall

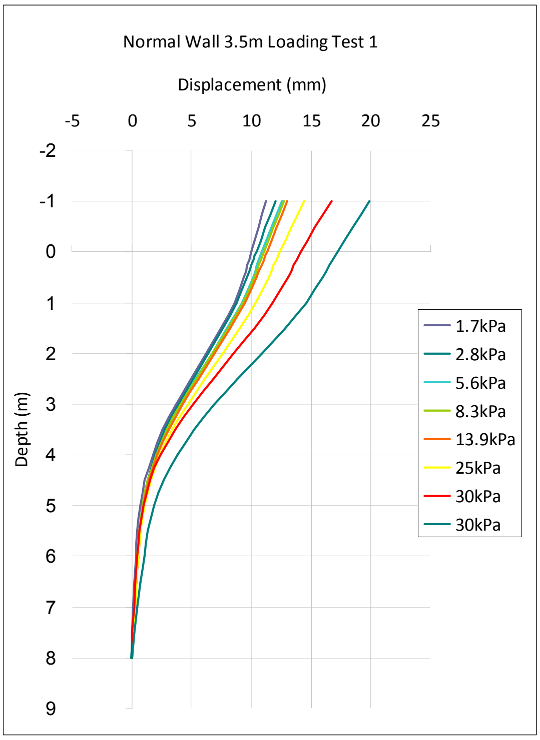

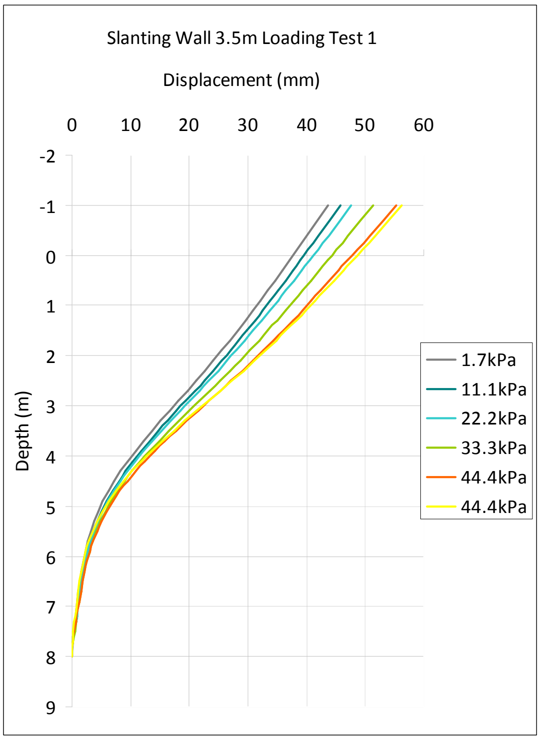

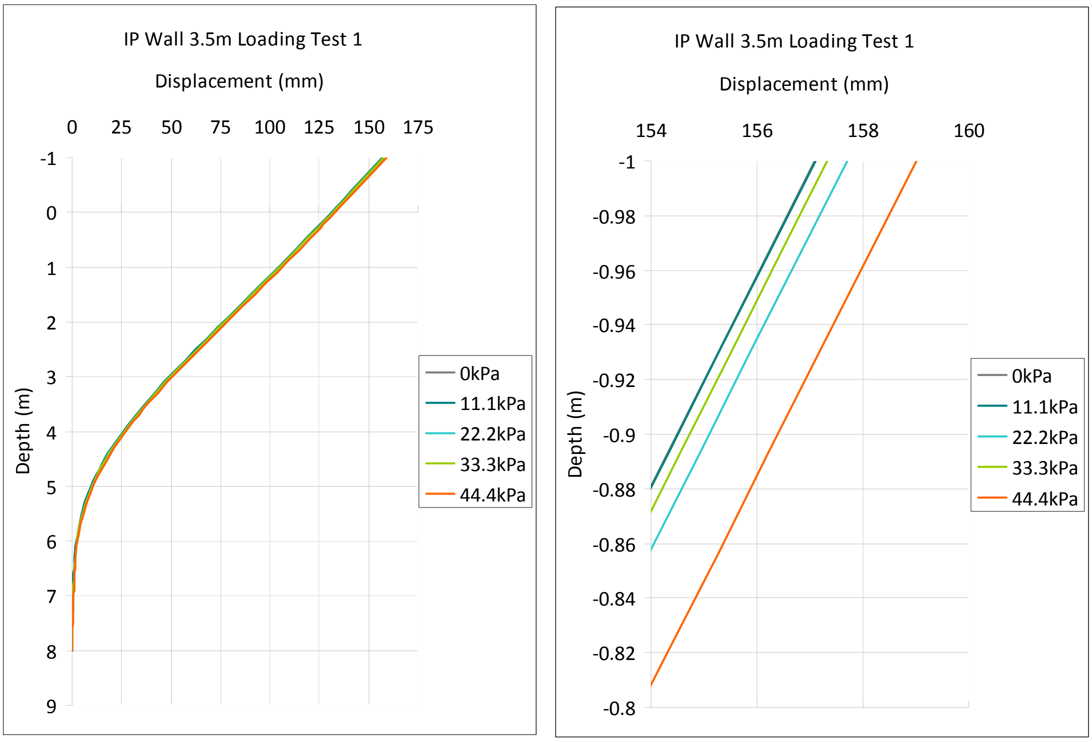

Fig.33 First Loading Test at 3.5m for Normal Wall, Slanting Wall and IP Wall

From Fig.33, it is obvious that IP wall experienced a far less displacement during loading. Normal wall have had a loading test at 3m, though excavation down to 3.5m was expected to cover the displacement due to 3m loading test. Normal wall resulted in more than 8mm of displacement under a maximum surcharge of 30kPa, while slanting wall gave approximately 20mm of displacement under a maximum surcharge of 44.4kPa. IP wall under the same maximum surcharge as slanting wall resulted in a displacement of 2mm, which is far less than the other two walls. Clearly, preload has stiffened the soil under the IP wall and will results in far less lateral displacement during loading.

Nevertheless, IP wall suffered from large wall movement during preloading, as shown in Fig.34.

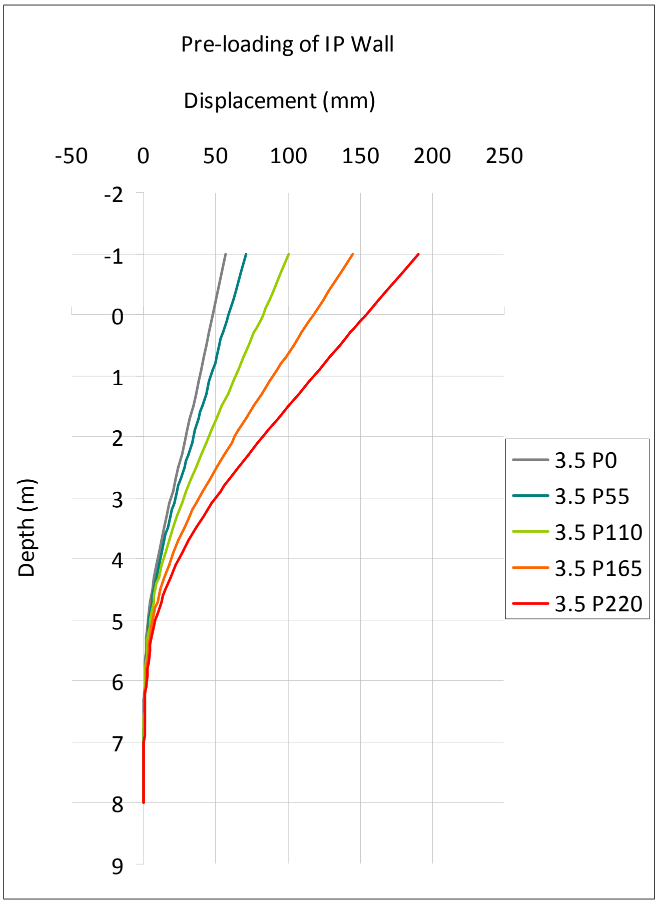

Fig.34 Pre-loading of IP Wall at 3.5m excavation; Magnitude of pre-loading increases from 0 to 220kN.

Pre-loading of IP wall added around 133mm to total displacement of IP wall. Although pre-loading improves the performance during service, the large deflection during the pre-loading process will limit the use of IP wall to a large extent. IP wall can only be applied to cases where lateral displacement during service should be minimised while wall movement during construction does not matter significantly.

7. Conclusion

The purpose of this report was to investigate the reliability of using existing theories to predict practical behaviour of sheet pile wall and to compare the performance of three different types of sheet pile walls. To assist with the research, three model tests and three field tests at the Akaoka test site was conducted from June to November, 2013. The main conclusions drawn from experimental data processing has been proposed as following:

● TS, strain gauge and inclinometers were able to collect relatively reliable and consistent data from field tests. Earth pressure sensor was found to be more sensitive and susceptible by other factors such as bending of the pile itself, and thus less reliable when pile is significantly bent.

● With reasonably defined values of soil parameter, the theoretical models using MSD and LED were found to be good predictions of lateral displacement of sheet pile wall during excavation. Nevertheless, a number of parameters for soil and sheet pile wall are difficult to measure in real field test. Instead of accurately prediction of wall movement, MSD and LED can be used for anticipate the possible range of wall deflection by assuming a range of input parameters.

● Theoretical models using MSD and LED tend to over-predict the displacement during loading tests.

● Soil parameters including angle of friction, soil type, and undrained shear strength, site condition such as the water level, together with the status of the sheet pile wall such as coefficient of joints and initial shape was found to significantly influence the lateral displacement of the sheet pile wall.

● Soil parameters including g_r, g_e, $\gamma_{m=2}$ together with the power a and b, have little effect on pile lateral displacement.

● IP wall was found to experience a far less lateral displacement in service due to the pre-loading. However, it was more likely to suffer from significant wall movement during the pre-loading process, which limits the application of IP wall to some extent.

● Further investigation is required to validate the mechanisms and models proposed in this report.

8. Future Work

Based the field test results in summer of 2013, suggestions for domains of further research into performance of sheet pile wall are:

● The Matlab model based on MSE can be developed to take initial shape, inclination of the wall and water level into consideration.

● The potential of pre-loading a sheet pile wall to increase its wall stiffness was clearly recognised in this project. The potential problem of large displacement during pre-loading was also identified. Further research on reduction in displacement during pre-loading would broaden the application of IP wall to a great degree. In addition, further quantitative research into precise displacement control by pre-loading is required before apply the IP wall into practical projects.

● More detailed investigation on influence exerted by initial pile wall shape and joint coefficient is of particular interest. Techniques to precisely control the initial shape and connection of sheet piles is worth research based on this report.

9. References

A. V. D. Bica and C. R. I. Clayton. Limit Equilibrium Design methods for free embedded cantilever walls in granular materials. Proc. Instn Ciu. Engrs, p 879-898, 1989.

W. Bjureland. Analysis of deep excavations using the mobilized strength design (MSD) method. Master's Thesis, Division of Soil and Rock Mechanics , Royal Institute of Technology, 2013.

M. D. Bolton, S. Y. Lam, and A. S. Osman. Supporting excavations in clay - from analysis to decision-making. 6th International Symposium on Geotechnical Aspects of Underground Construction in Soft Ground, IS-Shanghai, Vol. 1, 12-25, 2008.

M. P. Byfield and R. J. Crawford. Oblique bending in U-shaped steel sheet piles. Proceedings of the ICE - Structures and Buildings, Volume 156, Issue 3, p 255 –261, 2003.

M. Diakoumi and W. Powrie. Mobilisable strength design for flexible embedded retaining walls. Ge´otechnique 63, No. 2, p 95–106, 2013.

L.B. Feagin and M. AM. Soc. C. E. Lateral Pile-Loading Tests. American Society of Civil Engineers. Paper No. 1959, 1852.

S. O. Franklin and A. L. Olopade Observations on the Design of a Typical Anchored Sheet Pile in Cohesionless Media using the Conventional CECP2 and the BS8002 Design Methods. J. Basic. Appl. Sci. Res., 2(5)4571-4576, 2012

L. Grande. Some aspects on sheet pile wall analysis, soil structure interaction. Cost C7, Darmstadt, Oct.8-9, 1998.

S. Haigh and G. Madabhushi. Discussion of “Performance of a transparent flexible shear beam container for geotechnical centrifuge modelling of dynamic problems by Ghayoomi, Dashti & McCartney”. Soil Dynamics and Earthquake Engineering, 2014.

J. Han and D. Leshchinsky. Limit Equilibrium and Continuum Mechanics-based Numerical Methods for Analyzing Stability of MSE Walls. 17th ASCE Engineering Mechanics Conference, University of Delaware, 2004.

Y. Ishihara, N. Ogawa and K. Okada. Presentation about the Giken- Cambridge Collaboration, 2013.

P. Jacobs. Simplified Description of the Use and Design Methods for CPTs in Ground Engineering. PAJ Jul, 2004

K. K. Kim, M. Prezzi and R. Salgado. Interpretation of Cone Penetration Tests in Cohesive Soils. Purdue e-Pubs, 2006

M. Motoyama and T. L. Goh. Press-in Piling Technology: Development and current Practice. In International Workshop on Recent Advances in Deep Foundations, Yokosuka, Japan, 2007.

Norges Geotekniske Institutt. Norwegian Geotechnical Technical Report No.6. Oslo University Press, 1962

N. Ogawa. Presentation on 2013 Giken-Cambridge Collaboration Plan, Meeting of Giken-Cambridge Collaboration, 2013

K. Okada. Presentation on Model Test Results. Meeting of Giken-Cambridge Collaboration, 2013.

A. S. Osman and M.D. Bolton. Avoiding Excessive Displacements: A New Design Approach for Retaining Walls. International Conference on Structural and Foundation Failures Singapore, 2004.

P. Osório, C. Odenbreit and T. Vrouwenvelder. Structural Reliability Analysis of Quar Walls with Steel Sheet Piles. PIANC MMX Congress, Liverpool, UK, 2010.

S. Oztoprak and M. D. Bolton. Stiffness of sands through a laboratory test database. Ge´otechnique 63, No. 1, p 54–70, 2013.

R. Rajapakse. Geotechnical Engineering Calculations and Rules of Thumb. Butterworth-Heinemann, 2004.

Z. Rémai. Correlation of undrained shear strength and CPT resistance. Periodica Polytechnica Civil Engineering, p39-44, 2013.

P.K. Robertson. Estimating in-situ state parameter and friction angle in sandy soils from CPT. 2nd International Symposium on Cone Penetration Testing, Huntington Beach, USA, 2010

P.K. Robertson. Soil behaviour type from the CPT: an update. 2nd International Symposium on Cone Penetration Test, 2010.

P.K. Robertson and K.L. Cabal. Estimating soil unit weight from CPT. 2nd International Symposium on Cone Penetration Test, 2010.

B. Rymsza and K. Sahajda. Static Analysis of Restrained Sheet Pile Walls. 11th Baltic Sea Geotechnical Conference, Gdansk, Poland, 2008.

Y. J. Shin and D. Kim. Assessment of Undrained Shear Strength based on Cone Penetration Test (CPT) for Clayey Soils. KSCE Journal of Civil Engineering 15(7):1161-1166, 2011.

B. Simpson and W. Powrie. Embedded Retaining Wall: Theory, Practice and Understanding. Perspective Lecture, 15th International Conference on Soil Mechanics and Geotechnical Engineering, 2001.

I. Smith. Lecture on Retaining Walls and Geotechnical Design to Eurocode 7.

P.J. Vardanega and M.D. Bolton. Strength mobilization in clays and silts. NYC Research Press. 2011.

D. J. White and A. D. Deeks. Recent research into the behaviour of jacked foundation piles. In International Workshop on Recent Advances in Deep Foundations, Yokosuka, Japan, 2007.

P. I. Yakovlev. backfill stresses and earth pressure on sloping wall. Hydrotechnical Construction, Volume 8, Issue 12, p 1137-1142, 1974.

W. L. Yu, J. Zhang, R. L. Hu, Z. Q. Li, X. H. Sun and T. L. Li. Estimation of the Active Earth Pressure with Inclined Cohesive Backfills: the Effect of Intermediate Principal Stress is Considered. The Open Civil Engineering Journal, volume 5, p 9-16, 2011

10. Health and Safety

As the field tests were complete at the Akaoka test site in Kochi in the summer of 2013, no risk assessment about the experiments was submitted to engineering department. Nevertheless, during the field tests, Japanese health and safety regulations and standards were fully obeyed by all the members in the group. A health and safety induction was given to all members involved in the site work and other visitor engineers prior to any activities on site. Personal Protective Equipments were equipped according to relevant regulation.

Procedures of experiments and division of labour was discussed and decided every morning before the site work to ensure every member understand their own job. A meeting is held everyday after the experimental work to summarise the daily results. This was of significant importance to avoid any safety problems and accident due to the language barrier. A safety zone was clearly marked out when the craning work is going on.

Since Kochi is an area under seismological threat, tsunami and earthquake education was given soon after our arrival. The location of shelter and escape routes from the work site, the office and the hotel we live were clear shown to us on a map. Finally, the four-week site week finished without injury.

After the experimental work and on return to Cambridge, the health risk has become the prolonged computer use. Correct posture of seating was ensured during the data analysis and written up. All project works were done in a suitable working environment and breaks were taken every hour. No health problem was caused during the project.

11. Appendix

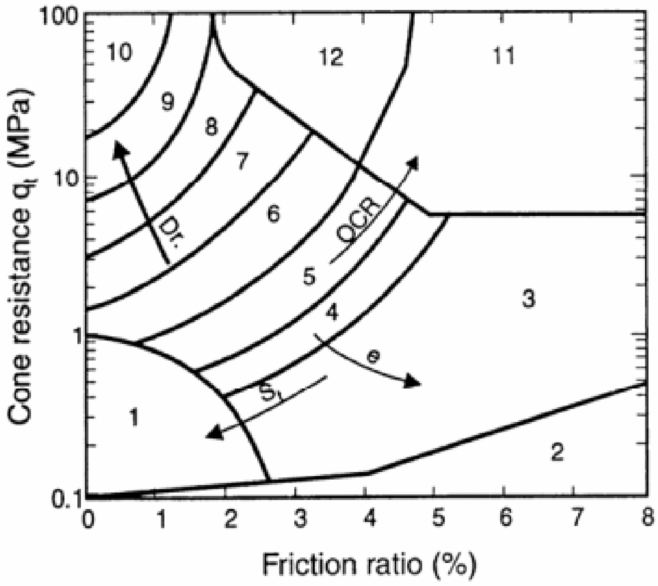

Zone	*Soil Behavior Type*
1	*Sensitive fine grained*
2	*Organic material*
3	*Clay*
4	*Silty Clay to clay*
5	*Clayey silt to silty clay*
6	*Sandy silt to clayey silt*
7	*Silty sand to sandy silt*
8	*Sand to silty sand*
9	*Sand*
10	*Gravelly sand to sand*
11	*Very stiff fine grained**
12	*Sand to clayey sand**

** Overconsolidated or cemented*

Fig.35 Correlation Chart of Soil type and CPT Measurements (Robertson, 1990)

Density index	Cone resistance (q_c) (from CPT) MPa	Effective angle of shearing resistance[a], (φ') °	Drained Young's modulus[b], (E') MPa
Very loose	0,0 – 2,5	29 – 32	< 10
Loose	2,5 – 5,0	32 – 35	10 – 20
Medium dense	5,0 – 10,0	35 – 37	20 – 30
Dense	10,0 – 20,0	37 – 40	30 – 60
Very dense	> 20,0	40 – 42	60 – 90

[a] Values given are valid for sands. For silty soil a reduction of 3° should be made. For gravels 2° should be added.

[b] E' is an approximation to the stress and time dependent secant modulus. Values given for the drained modulus correspond to settlements for 10 years. They are obtained assuming that the vertical stress distribution follows the 2:1 approximation. Furthermore, some investigations indicate that these values can be 50 % lower in silty soil and 50 % higher in gravelly soil. In over-consolidated coarse soils, the modulus can be considerably higher. When calculating settlements for ground pressures greater than 2/3 of the design bearing pressure in ultimate limit state, the modulus should be set to half of the values given in this table.

NOTE This example was published by Bergdahl et al. (1993). For additional information and documents giving examples, see X.3.1.

Fig.36 Derive Angle of Friction and Drained Young's Modulus from Cone Penetration Resistance (from Eurocode7-2)